Diagnostics and prognostics of planetary gearbox using CWT, auto regression (AR) and K-means algorithm

Manarikkal, I., Elasha, F. & Mba, D.

Original citation & hyperlink:
Manarikkal, I, Elasha, F & Mba, D 2021, 'Diagnostics and prognostics of planetary gearbox using CWT, auto regression (AR) and K-means algorithm', Applied Acoustics, vol. 184, 108314.
https://dx.doi.org/10.1016/j.apacoust.2021.108314

DOI 10.1016/j.apacoust.2021.108314
ISSN 0003-682X

Publisher: Elsevier

Diagnostics and Prognostics of Planetary Gearbox using CWT, Auto Regression (AR) and K-Means Algorithm

Imthiyas Manarikkal
Future Transport and Cities Research Centre
Coventry University
Coventry, United Kingdom
manariki@uni.coventry.ac.uk

Faris Elasha
Future Transport and Cities Research Centre
Coventry University
Coventry, United Kingdom
ac1027@coventry.ac.uk

David Mba
Department of Technology
De Montford University
Leicester, United Kingdom
david.mba@dmu.ac.uk

Abstract

Condition monitoring of machine is recognized as effective strategy for undertaking the maintenance in wide variety of industries. Planetary gearbox is a critical component in helicopters, wind turbines, hybrid vehicles and so forth. Planetary gearbox are complex in nature due to its size and meshing components. Condition monitoring and fault diagnosis of planetary gearbox is challenging due to complexity in dependable fault extraction from raw vibration signal. The mechanism of planetary gearbox is complex as there are several gears meshing at the same time. To find out the nature of fault and defective component in planetary gearbox is difficult. In this paper, the fault detection and fault type identification diagnostic approach using auto regression model (AR) and continuous wavelet transforms (CWT) by considering different frequency range is established. The experimental research conducted with different type of fault vibration signals in the gearbox have been diagnosed and identified the fault type using AR Modelling, Impulse and Shape Factor for validation purposes. The unique behaviors and fault characteristics of planetary gearboxes are identified and analyzed. The fault frequency identification and extraction of features from the non-stationary signals in different fault severity level of vibration data demonstrates the reliability of proposed method. The developed algorithm adds efficacy in detecting the nature of fault and defective component without performing a visual inspection.

Keywords
Condition monitoring
Auto regression modelling
Continuous wavelet transforms
Fault classification
Prognostics
Diagnostics

I. Introduction

Gears are designed to have infinite life and are one of the critical components in rotating machinery. Planetary gears are widely used in industry due to their co-axial shafting and high torque to weight ratio. The unexpected failures of planetary gearboxes will lead to increased downtime and structural damage. The condition monitoring of planetary gearboxes has received intensive research in the past decade due to its demand in heavy industrial applications [1][2]. It is very important to diagnose the early degradation of gears and bearings to prevent catastrophic accidents and production loss. Planetary gearboxes are exposed to varying loads and excessive stress conditions on the gear teeth. Therefore, gear tooth defects are one of the main causes of planetary gearbox failure. In the last 30 years, methods for detecting the early stages of faults in gears as well as bearings have been established by various researchers [2].

Vibration-based condition monitoring is manifestly the most common technique for fault diagnostics in rotating machineries. As a matter of fact, the early fault vibration signal from a gearbox is heavily corrupted with noise [3]. Therefore, a very sensitive fault detection and diagnostics method is needed to identify the early gear failure information [4]. Composite motion induced by multi-gear meshing results in time-variant vibration propagation pathways. This results in a distinctive non-stationarity in the dynamic reaction of the planetary gearbox. Its vibration spectrum is composed of various components conditions within the system during non-stationary operation, which renders the control of the conditions a challenging problem [5]. Different approaches have been used for the vibration based fault diagnosis of gears, Algorithms based on Fast Fourier Transform (FFT) and spectral methods such as Autoregressive (AR) time series models are among the most used ones. For instance, spur gearbox fault identification using a new integrated method based on AR model spectral estimation, principal component analysis and FFT has been developed by researchers [6][3] in the past. When different faults mutually exist in a gear system, the first task after fault detection is to classify the fault types. The fault classification method was also established from the feature vectors extracted using wavelet transform and AR model[Ref]. The AR model and cyclo-stationary analysis was also applied for fault identification in epicyclic gearboxes used in cranes. On method which helps identifying local fault in gears and reduction of noise effect on the signals is Time Synchronous Averaging (TSA). The analysis method adopted in this model is (TSA) for extracting the residual signal containing pertinent fault signatures [7][8]. Statistical features extracted from vibrations signals have notable use in gear fault detection. The statistical condition indicator and comparisons were established for studying the behavior of the gears during pitting cases. In most of the cases, the vibrations from gear systems are non-stationary. In such cases, Wavelet-based methods can be utilized to analyze signal spectrum. The fault detection of internal combustion engine gears using vibrational analysis and wavelet transform was established by Vernakar [9][10]. The research was conducted with a spur gearbox and picked peak frequency ranges for identifying faults, arguing that continuous wavelet transforms (CWT) is an effective tool for gear fault detection.

CWT are widely used because of their efficiency in identifying transitory and non-stationary signals. However, due to overlapping, the exact wavelet genetic method fault diagnostic method has been established and proven to be an effective tool for fault identification by minimising the undesirable overlapping effect in the spectrum [11]. On method that is generally used for the fault detection and isolation, is Artificial Neural Network (ANN). The main use of ANN is to find a model of a system for which the inputs and outputs are known. It can also be used for fault classification. The spur bevel gearbox fault detection using discrete wavelet transform and classification of fault types was implemented using the artificial neutral network (ANN) in the study conducted by Saravanan and Ramachandran [12]. It has been demonstrated that Time Synchronous Averaging (TSA) is a suitable technique for the extraction of features from the vibration signal in order to provide the state of a planetary gearbox during non-stationary operations [13]. The actual features were derived from the raw signal and the TSA signal to determine the health of the machine. However, it could be challenging to distinguish the early stages of harm by utilising TSA alone. It is often desirable to incorporate TSA with other methods, such as auto-regressive (AR) modelling, in order to increase the detectability of gear faults [14][15].

Raw vibration signals can be inspected in two ways: the classical method and the Artificial Intelligence (AI) method. Nowadays, with the help of technological advancements, the signal processing techniques have been shifted to intelligent systems, but the limitation of intelligent systems is feature extraction [16][17]. On the other hand, the apparent problem in rotating machineries is that vibration signals include a broad variety of normal and unstable frequencies owing to the intermittent actions of the system, so the detection of large frequencies within a small-scale diagnostic pattern is still a difficulty in signal processing [18]. CWT processes the vibration signals of the gearbox better than discrete wavelet transformation (DWT), since the down-sampling of the signals using DWT will result in the loss of significant details. The irregularity in the signal is one of the discriminating natures of pattern recognition. Fault detection using

FFT (Fast Fourier Transform), also known as global transformation, has its own limitations such as identifying the short duration signal and achieving better resolutions [19]. Wavelet functions will clear this gap in FFT by using functions that are scaled and shifted time-localized mother wavelets. It decomposes the signal in both time and frequency in terms of wavelets. CWT is used to create a time-frequency signal representation that offers very strong time and frequency localisation [20]. Lin and Qu [21] developed a novel method using the Morlet wavelet for identifying faults in a gearbox without de-noising. However, the researchers state that the continuous wavelet transform is an effective tool [22][23] for inspecting the residual signals and localisation of faults in gearboxes. For example, diagnostics of planetary gearbox using wavelet analysis with time synchronous averaging have studied by [51][52]. Auto regression (AR) modelling approaches which are parametric models, are ideal for identifying the fault level and also for comparing healthy vs. non-healthy rotating equipment. The superior resolution capability of AR models makes fault identification much easier and each data point of the signal is essentially connected to a series of previous data points utilizing certain coefficients (getting bigger with ageing) [24]. The power spectral density variations in gearbox signals contain a wealth of information [25]. The AR method is capable of detecting peaks (Gear Mesh Frequency (GMF) and its harmonics) [26] in the spectra compared to other well-known parametric methods such as moving average (MA) and AR moving average (ARIMA). Fault diagnosis of bearings and gears using K-means classification method and probabilistic neutral network algorithm have been performed very little in the past [46][47].

Prognostics is one of the valuable and challenging aspect of integrated structural health monitoring (ISHM) [48]. An efficient prognostic tool implies monitoring of health, life cycle and predominantly it is a safety factor. Prognostic tool can determine the hidden evolving fault, the RUL [49] and maintenance planning. The fault arises in gearbox over the period of its lifecycle are often destructive and increase the downtime. Prognostics will help to determine what will happen in the future and how to avoid catastrophes. There are mainly four types of prognostics; reliability based, physics based, data driven and hybrid approach. The data driven prognostics approach need enormous amount of data to process for estimating the future condition of the system. Despite the complexity of the prognostics, most of the approach uses accelerated test. Over the past few years, hybrid attention have caught much attention for remaining useful life prediction of planetary gearbox [50]. Run to failure data collection of machines are often hurdle for predicting the future life. Hence a data mining using machine learning techniques is useful in future prognostics field when there is only limited amount of data available for researchers.

This research proposes a diagnostic tool in case of different severity levels in a single stage planetary spur gearbox and a novel prognostic tool for estimating the severity and crack depth using 6D AR-K-Means model. The experimental data secured from healthy and non-healthy planetary gearboxes have been analyzed by considering different fault conditions and performing fault detection techniques using the AR method. The autoregressive (AR) model-based diagnostic approach utilizes an AR model of the gearbox signal as a linear prediction filter. For gear fault diagnosis, the synchronous signal average is prepared by the AR filter with the fault data being contained in the residual signal. In fact, one of the effective fault related features is extracted from AR models and used as input to K-means classification method. The study constitutes the following parts: First, the acquired gearbox vibration data are analyzed using FFT and envelop analysis (extraction of the modulation of structural resonance) for identifying the frequencies of individual components inside the gearbox and its behavior during healthy and non-healthy states. The pretreatment of the analysis for de-noising the signal was carried out using discrete wavelet transforms. In the second part, the continuous wavelet transforms applied as a diagnostic method in this study considered two different frequency ranges for the detection of the type of faults in the gearbox. Then the fault related features extracted from the processed signals carrying only certain frequency bands obtained by CWT, are used as input for K-means classification

algorithm. Fault sensitive feature extracted from AR models provides more effective classification in terms of classifying fault severity levels. The applied diagnostic algorithm based on the CWT-AR model has shown that the model is efficient for effectively detecting and classifying fault severity level in the selected planetary gearbox. In the last part, it has been shown that the developed prognostic tool which is based on K-means and vibration based features, works pretty well in determining gear tooth crack severity level and prediction of the onset of the threshold value at which the gears need to be replaced.

II. PROPOSED ALGORITHM

Wavelet de-noising

The wavelet denoising or wavelet thresholding can preserve the important signal from white noise. The fault characteristics are often hidden in the spectrum obtained from the gearbox vibration data. The discrete wavelet transforms (DWT) are often used for minimising the negative influence of noise [6] in the spectrum that allows visibility over various fault frequencies. The periodic impacts of localised defects and the feature component of the signal can be extracted using DWT (decomposing the orthogonal set of wavelets) for capturing the mesh frequencies as well as other components characteristics frequencies [30]. DWT accordingly uses multi-resolution filter banks (biorthogonal) that are very effective in the analysis and reconstruction of vibration signals [31]. The DWT filter arrangement is represented in the figure 1 where the number 2 inside circles means downsampling or upsampling with a factor of two.

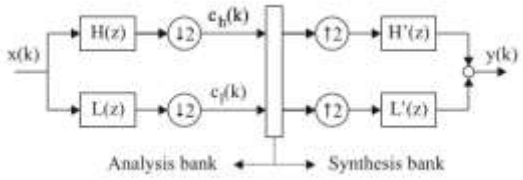

Fig. 1 Biorthogonal DW filter bank

The discrete signals enter the biorthogonal filter bank that contains the low pass $L(z)$ and high pass filter $H(z)$ and it separates the frequencies of the input signal in equal bandwidths.

AR Modelling

Autoregressive modelling is one of the prominent methods for fault diagnostics in gears and bearings. It is a stochastic tool for high resolution spectral estimation that can reliably show errors and deviations from the threshold. Variations of model coefficients and modelling errors can be used to detect the gears' and bearings' faults. In an AR model, the current value of a time series $x(n)$ or white noise at a discrete time instant (n) is expressed as follows below [14],

$$x(n) = -\sum_{k=1}^{p} a_k x[n-k] + e(n) \tag{1}$$

where the p is previous values, $e(n)$ is the error term and a_k is the autoregressive coefficients. The simple AR modelling transfer function is represented in the following figure which shows the input-outputs of AR model and the fact that is a discrete time transfer function based on z-transform.

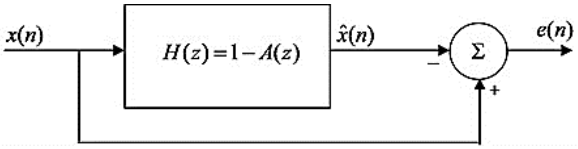

Fig. 2 AR prediction model

The residual (error) signal which has to be minimized in order to find AR coefficients, is represented as

$$e(n) = x(n) - \hat{x}(n) \tag{2}$$

.

Where $x(n)$ and $\hat{x}(n)$ denote the original signal and estimated signals. The estimation of the AR parameters can be achieved using various methods [25]. In this study, the proposed method of estimating the AR coefficient for arbitrary p on the autocorrelation matrix uses the Yule Walker equation [32].

Continuous Wavelet Transform (CWT)

Continuous wavelet transforms are a windowed infinite version of Fourier transform containing a merit function localised in real and Fourier space. The data obtained using CWT are contains all frequencies which makes it hard to analyze and detect fault signatures. It is possible to do the time-frequency decomposition using CWT, such that the transformed signal carries only a specific range of frequencies at which the fault signatures are more apparent.. The analyzing function is known as wavelets. The continuous wavelet transform can be defined as follows,

$$C(a,b) = \int_{-\infty}^{+\infty} f(t)\psi_{(ab)}(x)dt \tag{3}$$

where, $\psi_{(ab)}$ is a continuous function in both time and frequency domains called the mother wavelet which can generate a series of son wavelets, by dilation or scale (a) and translation or time location (b) [6, 21,27,28].

$$\psi_{a,b}(t) = \sqrt{a}\psi\left\{\frac{t-b}{a}\right\} \tag{4}$$

The time t and time-scale factor varies continuously [29]:

$$CWT\{x(t); a, b\} = \int_{-\infty}^{+\infty} x(t)\psi^*_{a,b}(t)dt \tag{5}$$

K-Means Clustering and Prognostics

K-means clustering is one of the unsupervised machine learning algorithms which uses vector quantization to classify the input data. There are four steps involved in K-means clustering technique. It is an iterative algorithm that tries to partition the dataset into *K*pre-defined distinct non-overlapping subgroups (clusters) where each data point belongs to only one group. In this algorithm, data points are assigned to the closest cluster based on a similarity measure (E-step, equation 6). Then the centroid of the cluster is calculated (M-step, equation 7).

It is actually minimization problem of two parts. We first minimize the performance function J with respect to the weights wik and treat μk fixed (equations 6 and 7). Then we minimize J with respect to μk and treat wik fixed. Technically speaking, we differentiate J with respect to wik first and update cluster assignments (E-step). Then we differentiate J with respect to μk and recompute the centroids after the cluster assignments from previous step (M-step). In other words, assign the data point xi to the closest cluster judged by its sum of squared distance from cluster's centroid.

The objective function is:

$$J = \sum_{i=1}^{m}\sum_{k=1}^{K} w_{ik}\|x^2 - \mu_k\|^2 \tag{6}$$

The E-Step is:

$$\frac{\partial J}{\partial w_{ik}} = \sum_{i=1}^{m}\sum_{k=1}^{K} w_{ik}\|x^2 - \mu_k\|^2 \tag{7}$$

Implies,

$$w_{ik} = \begin{Bmatrix} 1, \text{if } K = argmin_J\|x^2 - \mu_k\|^2 \\ 0, \quad \text{otherwise} \end{Bmatrix}$$

The M-Step is:

$$\frac{\partial J}{\partial \mu_k} = 2\sum_{i=1}^{m} w_{ik}\,(x^2 - \mu_k) = 0 \tag{8}$$

Implies,

$$\mu_k = \frac{\sum_{i=1}^{k} w_{ik} x^i}{\sum_{i=1}^{m} w_{ik}}$$

The re-computing of cluster centroid is using the following equation:

$$\frac{1}{m_k}\sum_{i=1}^{m_k}\|x^2 - \mu_k\|^2 \tag{9}$$

III. EXPERIMENTAL SET UP

The planetary gearbox with equally spaced planets are taken as research object. The gearbox is coupled with 3-phase motor to the sun gear (input), which is assembled with three planet gears. The planet gears are pinned to the arms of carrier gear (output) with needle roller bearing. The output shaft of the carrier gear is connected to the load motor by means of structural steel coupling shaft. The operating conditions of the test are illustrated in the table 1.The planetary spur gear and the planet bearings parameters are shown in Table 2 and 3, and their characteristics frequencies [33] are shown in Table 4. The vibration data is collected for 20s duration at a sampling frequency of 12800 Hz, given 256000 samples. During experiments, the rotating frequency of the drive motor connecting to the sun gear shaft is set to a constant speed of 23.33 Hz. The magnetic accelerometer (PCB Model 352C03) measurements are taken periodically from two different points (position 1: on top of the ring gear and position 2: near to the sun gear) for acquiring different voltage data sets. The maximum vibration based on position of sensor was found on top of the ring gear. The experimental set-up is shown in Figure 3. The healthy gearbox was initially tested and then faults were induced on the components. The vibration was

measured under three different conditions: 1- healthy, 2- pitting on the planet (artificially made by milling) and 3- a crack on the planet tooth case. During the analysis stage, it is very important to resample [34] the frequencies to alleviate the computational problem.

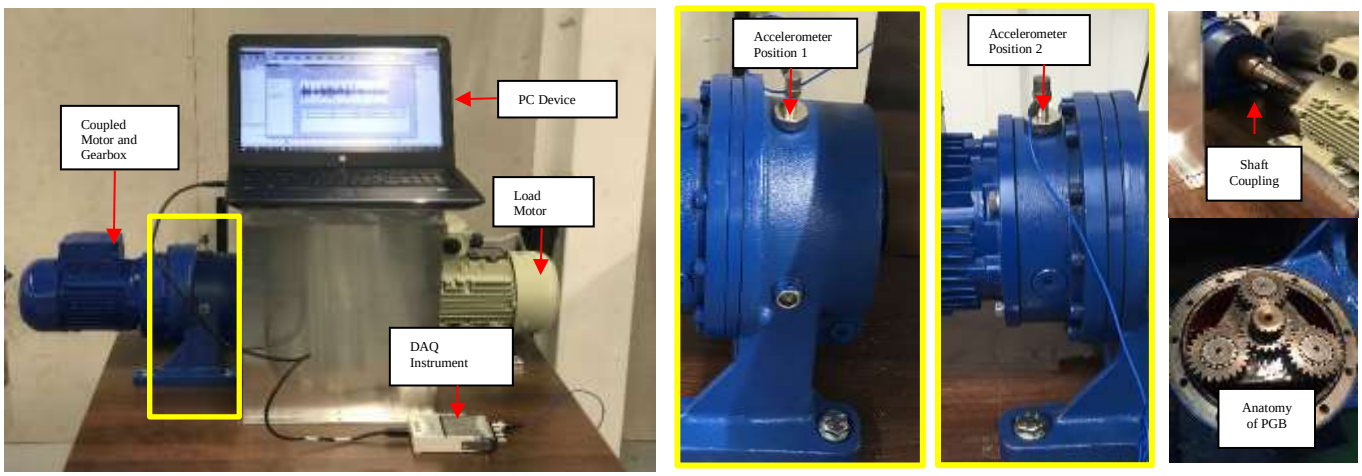

Fig.3 Planetary gearbox experimental test rig

Table 1. Operating conditions of the gearbox

Parameters	Sun (s)	Planets (p)	Carrier (c)	Ring (r)
No. of teeth (z)	23	24	-	73
Pitch radius	22.85mm	23	-	149mm
Mass	309g	1816g		1224g
P.A	20	20	20	20

Table 2. Parameters of PGB

Sampling Period	Input Speed	Output speed	Ratio	Operating voltage	Torque
12800 Hz	23.33 Hz	5.58 Hz	4.17	400v /3phase	10.2 Nm

Table 3. Planet Bearing Parameters

Planet Gear Bearing Specification			
No. of Balls N_B	Ball Diameter B_D	Pitch Diameter P_D	Contact angle β
16	4.94	10.94	0^0

Table 4. Characteristics frequencies of PGB components

	Characteristics frequencies equation	Characteristics frequency
GMF	$f_m = f_H . z_r = \frac{z_r z_s}{z_r + z_s} . f_s$	438.09 Hz
Sun	$f_s = \frac{z_r}{z_r + z_s} . f_s = \frac{f_m}{z_s}$	23.33 Hz
Planet	$f_p = \frac{z_r . z_s}{z_p (z_r + z_s)} . f_s = \frac{f_m}{z_p}$	17 Hz

Carrier	$f_r = \frac{z_s}{z_r + z_s} f_s$	5.58 Hz
Planet Needle Roller Bearings	$BPFO = RPM \times \frac{N_B}{2}(1 - \frac{B_D}{P_D}\cos(\beta))$	BPFO: 80.13
	$BPFI = RPM \times \frac{N_B}{2}(1 - \frac{B_D}{P_D}\cos(\beta))$	BPFI: 211.867

The arrangement of the planetary gearbox components is illustrated in the following figure. The input is the sun gear (2) coupled with the motor shaft. The output is the carrier gear (1) containing 3 planet gears and their associated bearing modules. The carrier gear is connected to the load motor with the shaft coupling. The ring gear (3) is arrested with the gearbox cage, which has no freedom of movement. The induced fault was made on one of the planet tooth for studies after several cycles gearbox in healthy condition. Then the fault severity was increased to confirm the effectiveness of the proposed diagnostic algorithm.

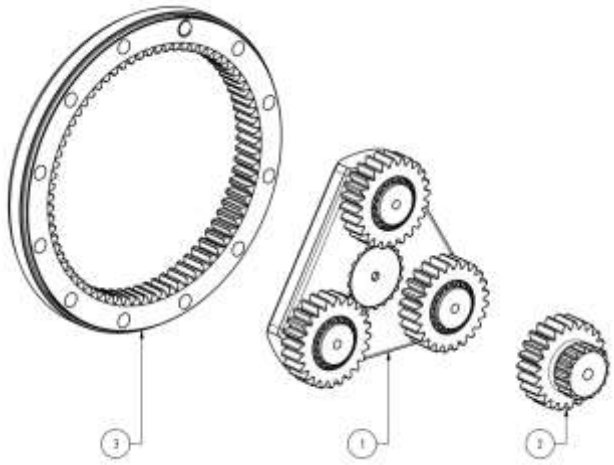

Fig.4 Single stage planetary spur reduction gearbox components arrangement.

IV. CASE STUDY

The measurement point is fixed on the ring gear. The influence of the sensor spinning in the vibration signal is neglected in this study. It is worth noting that the test rig is running at a constant output speed of 335 RPM or 5.58 Hz with a 10.2 Nm torque. If there is a fault present on the gears, there will be modulation effects in the vibration signal and also the defect will rotate with the carrier gear with a speed of f_d.The defects generally reveal themselves by the sidebands of the gear mesh frequencies that possess individual harmonics and frequencies. The modulations in the vibrations are often caused due to eccentricities, manufacturing errors, varying loads etc. A damaged tooth or defect in the bearing module can cause modulation when the gear passes through its mesh. The modulations are evenly spaced lines on either side of the center frequencies [35]. The modulation sidebands occur at specific frequencies of $f_m \pm n$, where f_m is the gear mesh frequency of the planetary gearbox and n is the integer according to the sideband energy ratio theory [36].

Generally, in the spectrum of the gear vibration, peaks appear at mesh frequency and its harmonics. Depending on the situation, the peaks at gear mesh frequencies may not be dominant [37]. In this study, the planets are equally spaced around the sun gear. If there is a

fault existing on the any of the gear teeth, there will be a variation in amplitude and phase in vibration. The occurrence of sidebands and the identification of fault location in the planetary gearbox components have been well studied by Liu et.al [38]

Fast Fourier Transform (FFT) is initially used as a basic analysis to study the fault signatures in the spectrum. Since the vibrations from different components are modulated and the fault signatures of different components such as gears and bearings reveal themselves in different frequency bands, the envelop analysis is used as well. The envelop analysis with Hilbert transform is performed to study the fault symptoms generated by bearing faults. This is an effective method for extracting the fault frequencies of gears and bearings at the same time, as per the researchers [39] [40].

The signals collected from the gearbox in different conditions are non-stationary and noisy. There is uncertainty in the meshing of the gears as well. Therefore a method for removing these effects and yet keeping the frequency content of the signal is vital. Time Synchronous Averaging (TSA) is applied on the signals for some faults to average out the effects other than the fault effect in the signal.In the FFT spectrum of the signals, the focus will be mainly on the gear mesh frequency and its harmonics. A change in the amplitude of vibration and the harmonics can reveal a change in the gear, i.e. a fault or resonance. Other than the vibration amplitude at harmonics, the sidebands around these frequencies carry useful information about gear system health. Therefore, these frequencies will be watched in the spectrum in detail.

When a planetary gear is faulty, in order to detect the fault, planet pass frequency (nf_c) is of high importance. The planet pass frequency in the system will cause asymmetric modulation sidebands around the gear mesh frequency and its harmonics. According to Huff and Tumer [41], a planetary gearbox with evenly spaced planets will not exhibit a dominant gear mesh frequency if the number of teeth on the ring gear (z_r) is not an integer multiple of the number of planets (n). In our case, the epicyclic gear mesh frequencies are suppressed in most cases because the number of teeth on the ring gear is not an integer multiple of the number of planets (73/3). The gearbox teeth are designed in such a way that the number of teeth are in prime numbers (so that the wear spreads very slowly). In our case, pitting is artificially generated on one of the gearbox's planet teeth. The pitting is on the line of contact region of the planet tooth. It is obvious that when the planet passes through the point of the accelerometer, it will excite the sensor on each planet pass frequency. Some of the gear fault identification techniques used in normal fixed shaft gears are also applicable in epicyclic gearbox fault identification. However, the carrier rotation and ring gear error sidebands will be visible in the epicyclic gearbox vibration spectrum.. In case there is an abnormal tooth load present in the gearbox, the first gear mesh frequency will be larger than the second and the third. When there is tooth wear or pitting present, multiples of harmonics can be found in the spectrum with high populated sidebands modulation.

The carrier gear (output) frequency can be taken as one of the references for identifying the nature of the fault in the gearbox. The carrier gear is pinned to the planet bearings and the planet gears mesh with the sun and ring gear produce torsional vibration that is mostly related to the gear mesh frequency. The higher harmonics at gear mesh frequencies are also related to backlash and time varying mesh stiffness. The damaged planet tooth will add additional frequency components and these components are often located in $\left(mz_r + q\frac{N_s}{N_p} + k\right)f_c$, where z_r is the number of ring gear teeth, N_s is the number of sun gear teeth, N_p is the number of planet gear teeth and f_c is the rotational speed of the carrier and m, q and k can be any integers. Existence of such frequency components may suggest that there is a fault present on the planet gear, [42][43][44].

The captured voltage signals from the accelerometer of a healthy and an unhealthy gearbox are represented in Figure 5. The AR model is applied to the signal acquired from the healthy gearbox to the gearbox with a gradually worn tooth. The suitable order n, for the signal

is found as $n = 56$. This is done by the minimization of estimation error and cross validation. The estimated model of the healthy gearbox is identified by the AR model (x_h) and compared with the original signal (x) after a 150 hours cycle and can be found in Figure 8.

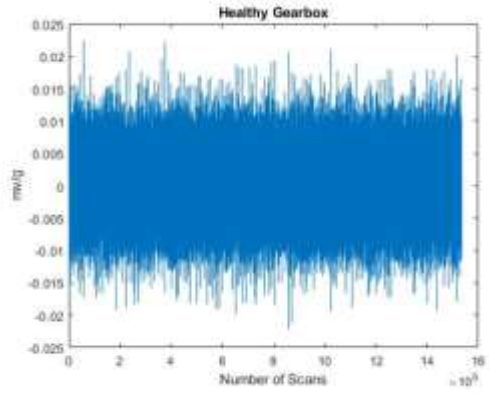

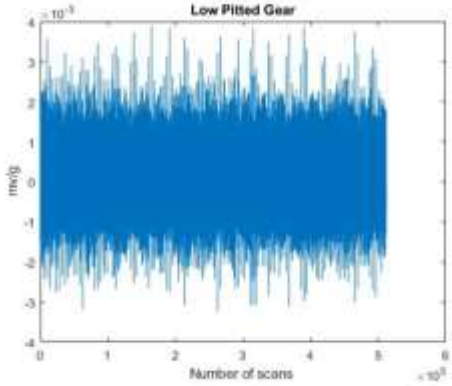

Healthy and Unhealthy signal

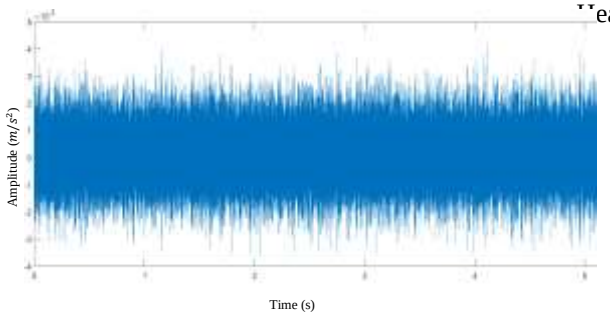

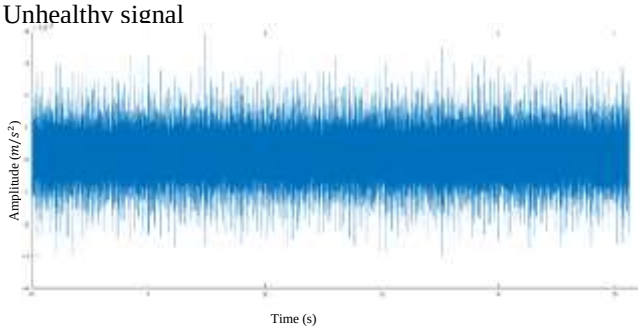

Fig. 6 Healthy gear signal

Fig. 7 Unhealthy gear signal

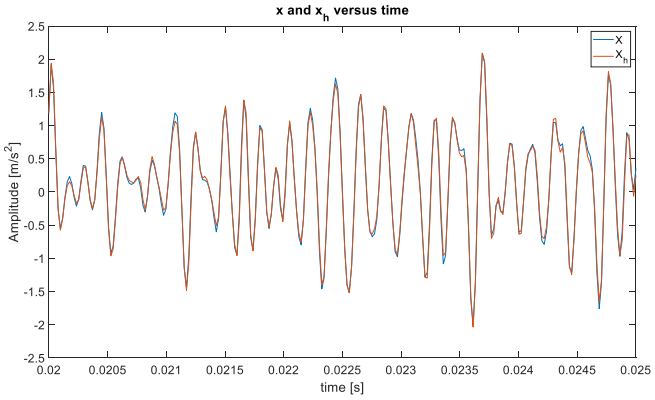

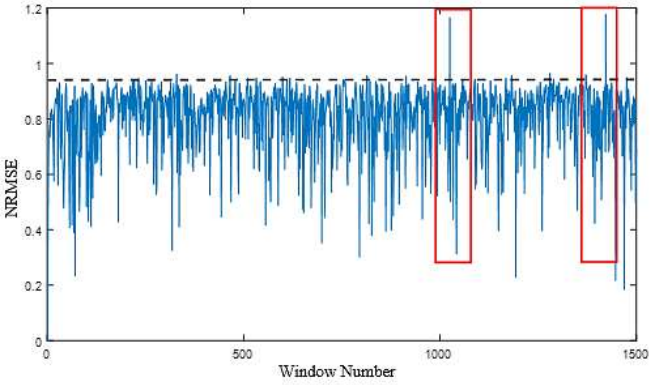

Fig. 8 AR Model signal prediction (x: original, x_h: estimated)

Fig. 9 NRMSE of AR model coefficients

AR method can be used to model the signals and out of the estimated models, fault related features can be obtained. These features can be a function of AR coefficients. Figure 9 shows the Normalised Root Mean Square Error (NRMSE) of the AR model coefficients, suggesting that there is a difference between the models for healthy and faulty signals. This shows a change and a fault can be detected. The aforementioned graph is obtained with a moving window of a length of 4096, meaning a moving window over the signal was applied and in the part of the signal which fault is effective, the change in the NRMSE of the modelled signal will be visible However, if a threshold of approximately 0.95 is set and again it can be seen that at two windows, the value goes beyond the threshold level, a

change and hence a fault is detected. Also, checking the other features suggests that all of them reveal a change once they are compared for healthy and faulty signals, especially the square root of amplitude (SRA), SF (Shape factor) and KV (Kurtosis value). These statistical features are used to strengthen the fault detection algorithm, as one of the features might be more sensitive to the fault than the others.

For detailed analysis and fault identification, fault features in the FFT signal such as sidebands can be further investigated. The inspection is mandatory if there is a fault alarm from the acquired signals.

Therefore, fault detection was performed using AR model. In the next step, to developa diagnostic method, an induced pitting has been made for further analysis (see Fig 10).

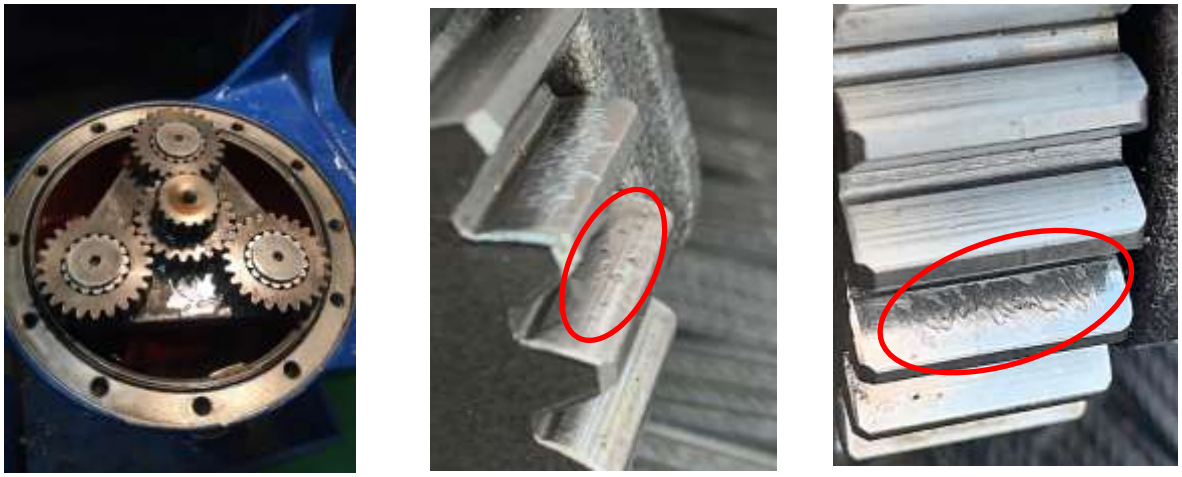

Fig. 10 Dismantled gearbox (left), natural pitting (middle) and induced pitting on the planet tooth (right)

In order to establish a robust algorithm for fault detection and fault classification, a set of fault sensitive features can be extracted and used. Here, the obtained features are SRA, SF and KV which show that the amplitude of vibration has increased drastically. In the following graphs, the red line denotes the sum of mean and standard deviation.

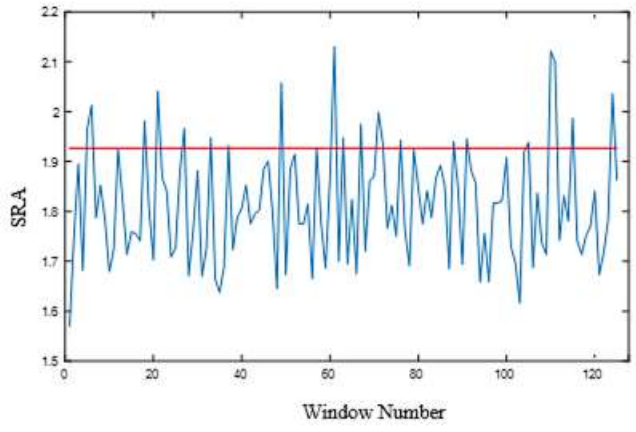

Fig 11 SRA of low frequency range of faulty gearbox

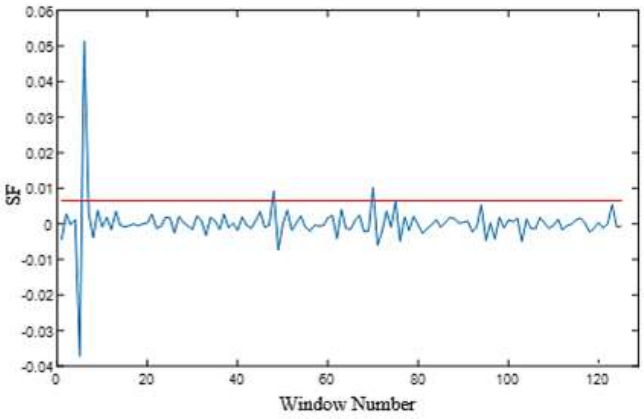

Fig 12 SF of low frequency range of faulty gearbox

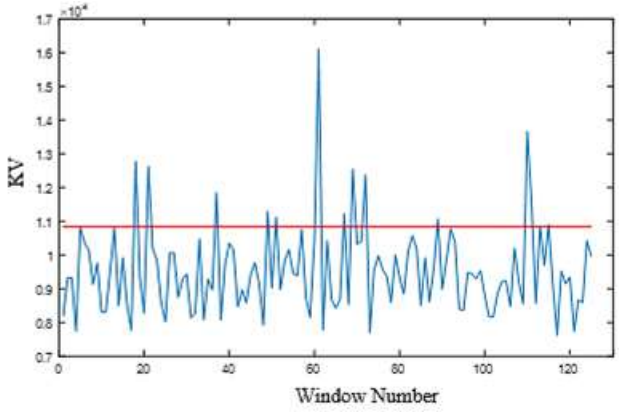

Fig 13 KV of low frequency range of faulty gearbox

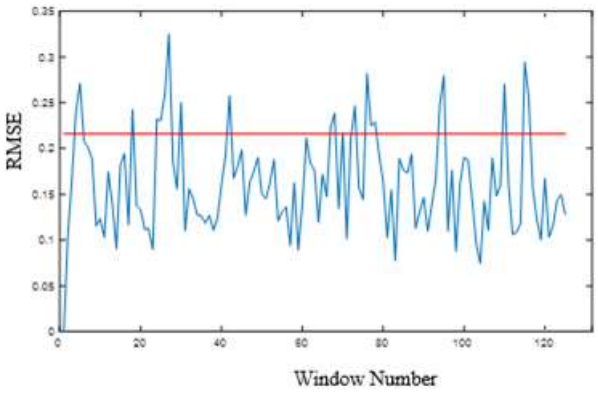

Fig 14 RMSE AR Coefficient in low frequency range of faulty gearbox

Using CWT, the analysis is performed for a data set carrying two different frequency ranges; the entire frequency range and the low frequency range. The results reveal that in most cases, the features show the fault more effectively in the case of low frequency signals. The vibration signature of the gear (in our case, its planet), under analysis can be separated from other sources of vibration using the TSA method. The TSA is carried out taking the carrier speed as reference. Furthermore, any shaft speed variations that give reliable and less uncertain results can be corrected using TSA. The FFT of the signal was performed after the TSA for fault identification by comparing the healthy and pitted gearbox cases. In what follows, the results of FFT analysis is presented. According to Figure 15, the FFT of the healthy gearbox has a dominant peak at the first and second gear mesh harmonics. Characteristic frequencies of the gearbox can be see in detail in the focused view in Figure 16. However, in the FFT of the pitted planet gearbox, the dominant peaks occur in higher harmonic with high amplitude, which is the 5^{th} harmonic here. As one may know, pitting is a localised fault and shows itself at the harmonics of mesh frequencies with sidebands related to the planet frequency (f_p). As can be seen in Figure 17, there are high peaks at planet frequency harmonics at a speed around the 5^{th} harmonic of mesh frequency and this is a clear indication of a localised fault in the planet. In the case of a healthy FFT spectrum there is no dominant peak at a high frequency with the corresponding sidebands. The

FFT in both cases is calculated using TSA signals, which are obtained by averaging with respect to the carrier speed (f_c). Therefore, we can say the sidebands ($3f_c$) are related to the carrier frequency.

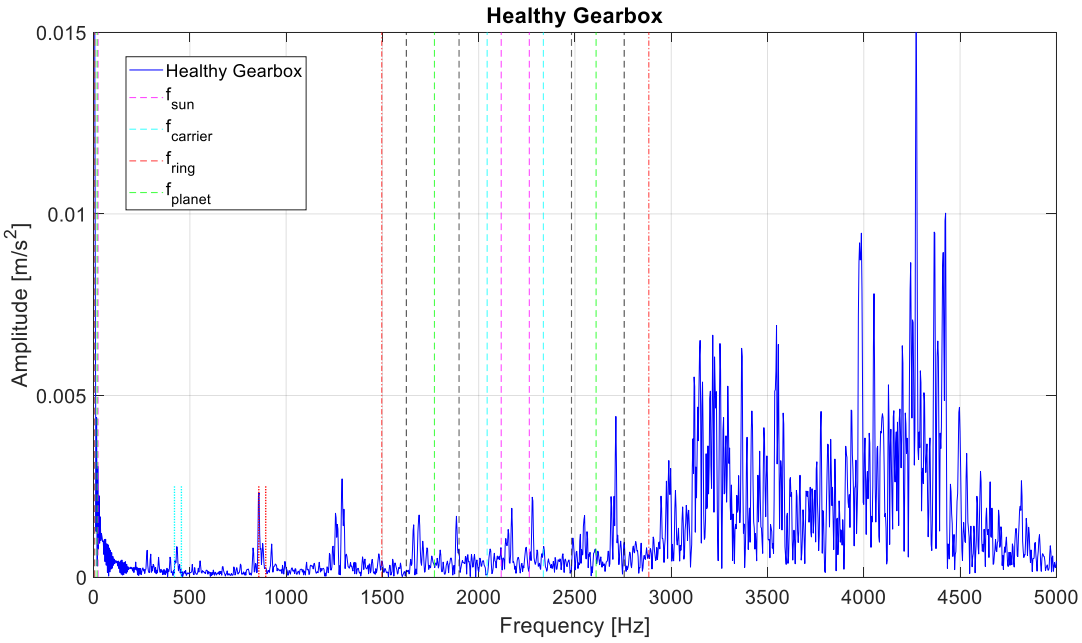

Fig. 15 Healthy gearbox FFT

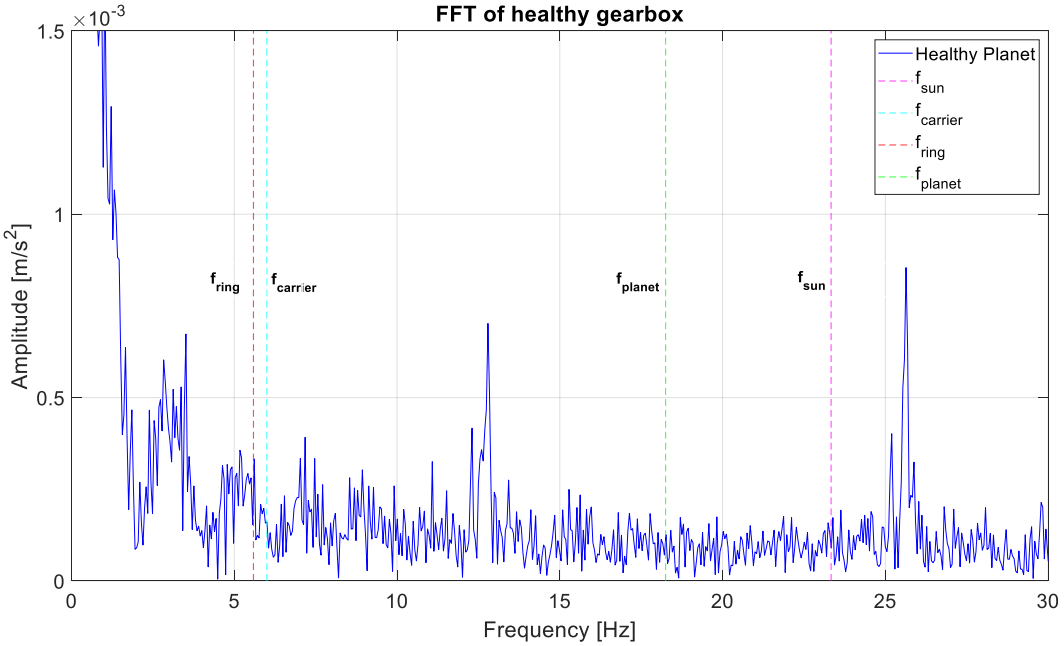

Fig. 16 Healthy gearbox FFT magnified.

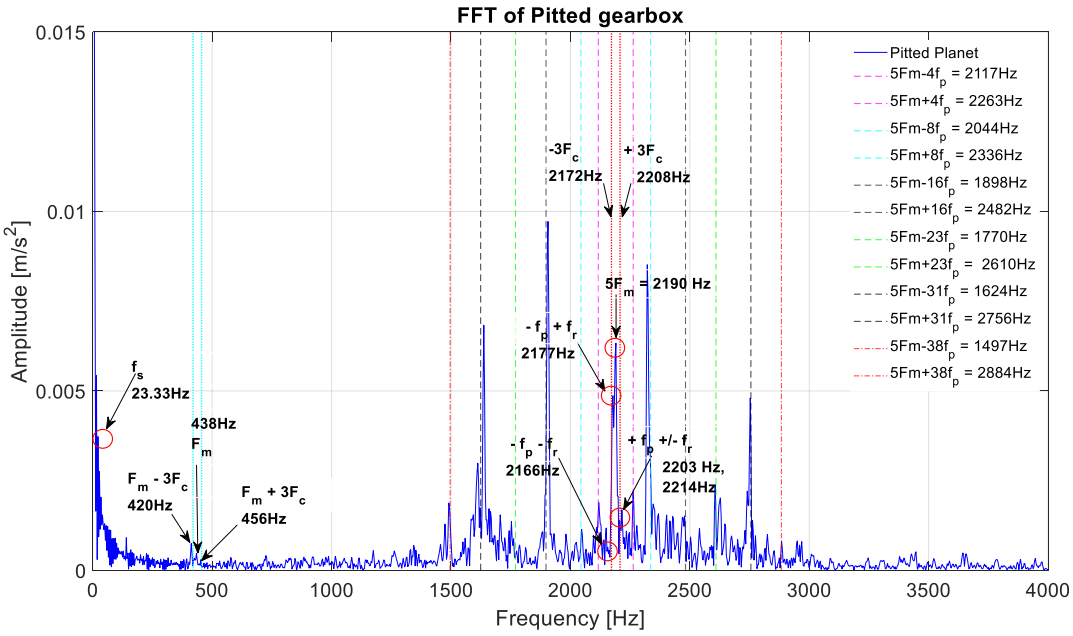

Fig. 17 Unhealthy gearbox FFT magnified.

After determining the fault from the TSA and FFT analyses by looking at the lower frequency range (0-2.5 kHz), the presence of gear mesh frequency harmonics peaks and its high amplitude sidebands indicate that a fault on a tooth. The next phase of the fault detection is to identify the characteristic frequencies of the individual components in the gearbox by envelop analysis using the Hilbert transform. The envelop analysis of healthy and unhealthy states can be found in Figures 18 and 19. The normal envelop analysis is effective for the fault detection of the bearing. Therefore, the Hilbert transform is used for detecting the submerged frequencies in envelop by removing the negative parts and doubling the magnitude of the positive part, so that clear peaks of the gears are identified in the spectrum for further analysis. The sidebands around the peaks at the envelop spectrum of the unhealthy gearbox resembles the fault in the planet.

However, there is no dominant peak at BPFO (80.13 Hz) and BPFI (211.86 Hz) higher harmonics. This indicates that there is no fault in the bearing modules of the planet.

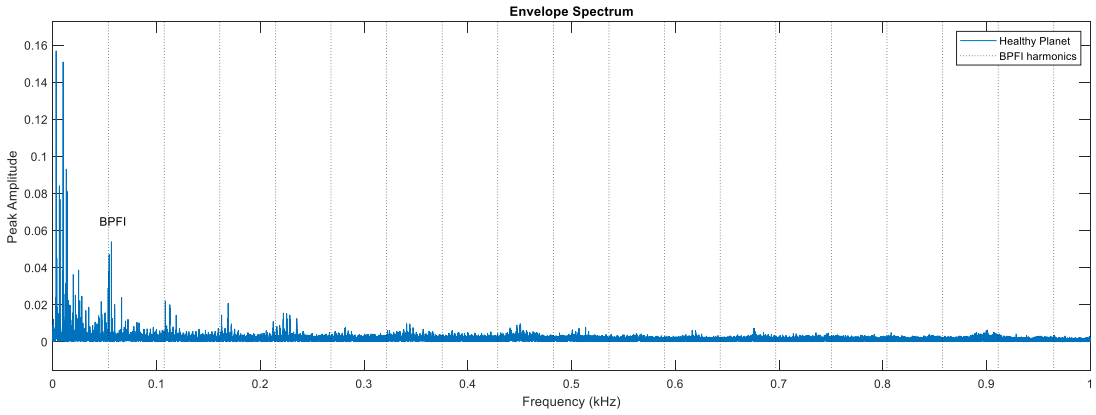

Fig. 18 Healthy gearbox envelop spectrum

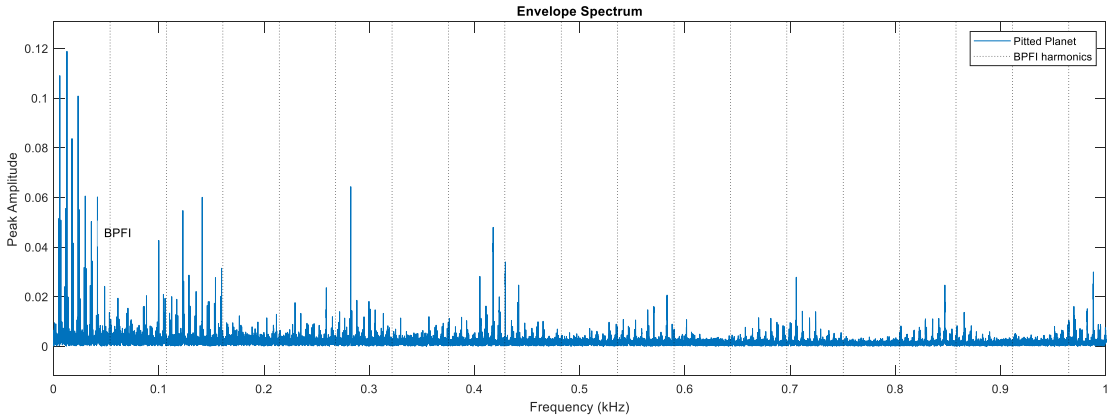

Fig. 19 Unhealthy gearbox envelop spectrum.

The continuous wavelet transform together with TSA is then performed for identifying the faulty component in the gearbox. If there is a distributed (wear or crack) or localised (pitting or spalling) fault present, there will be more energy distributed in certain frequency bands. For pitting faults, it is expected to have dominant peaks at high mesh frequency harmonics which repeat each time the planet passes through the accelerometer position. In order to discover the faults, CWT is obtained at different frequency bands over the length of the signal. Considering the healthy and pitted gearboxes at low frequencies, no dominant peaks have been observed (Figs. 20 and 21 b); whereas in the mid frequency range of an unhealthy gearbox (Fig. 21.c) there are clearly visible peaks that are repetitive over time. Each time the pitted planet tooth meshes through the ring gear, it produces an impulse on the ring gear where the accelerometer is mounted. We can clearly see this on the CWT unhealthy mid frequency spectrum. A pitting influence on the response is like a moving impulse. So, for one revolution of the carrier, the defected planet crosses the accelerometer once and we see high power (amplitude) at that point. Since the impulse reveals itself in a wide frequency band, we see it spread in a specific frequency band. Furthermore, the amplitudes of the dominant peaks decrease when the pitted planet moves far away from the accelerometer position. Similar to the FFT of the unhealthy gearbox spectrum, here the dominant peaks are located around the fifth gear mesh frequency (2-2.2 kHz).

The verification of the proposed method is essential to prove its contribution as an effective diagnosis tool for a planetary gearbox. Therefore, the crack on the same pitted planet tooth was induced to increase the fault severity for further analysis and verification. The following Figure 22 shows the induced crack on the planet tooth.

Considering the crack on the planet gear case tooth, the CWT figures show that the effect of the crack reveals itself around the second mesh harmonics, which is 875 Hz. Referring to Figure 21 c, at a low band frequency (100-1400 Hz), a series of peaks can be detected with high amplitudes. While the amplitudes are greater near the sensor location, their magnitude decreases when the cracked planet is moving further. Due to the repetitive pattern of the motion, this effect is magnified once TSA is applied on the signal. Since the crack is a distributed fault, its effect is rather long in time and narrow in frequency. So, the meshing of the cracked tooth occurs in a period which is longer than the mesh period. Therefore, other than the dominant peak at certain harmonics of the mesh frequency, a series of sidebands around a particular peak would be absurd [45]. In the lower frequency range, distributed peaks in time can be observed at a time between 20 to 40 seconds and this complies with our expectations of the crack's influence on the response.

Fig. 20 Healthy gearbox CWT of TSA acceleration

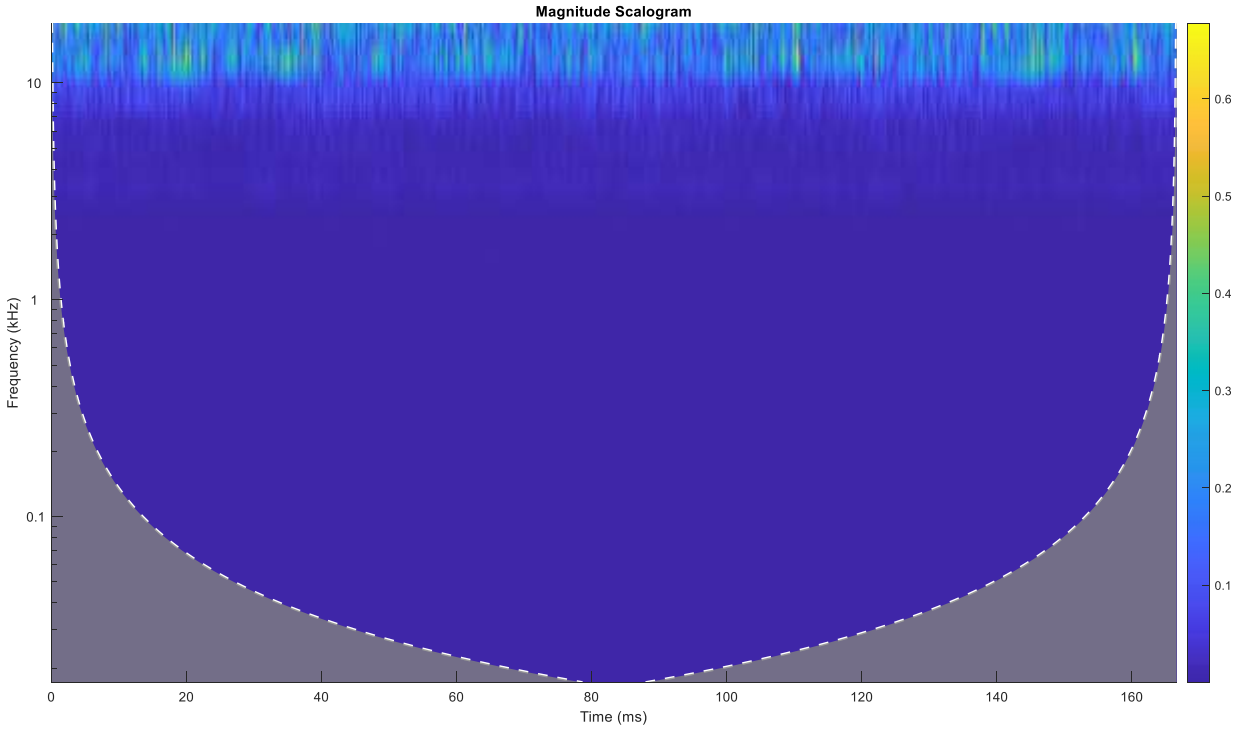

a) CWT of TSA pitted

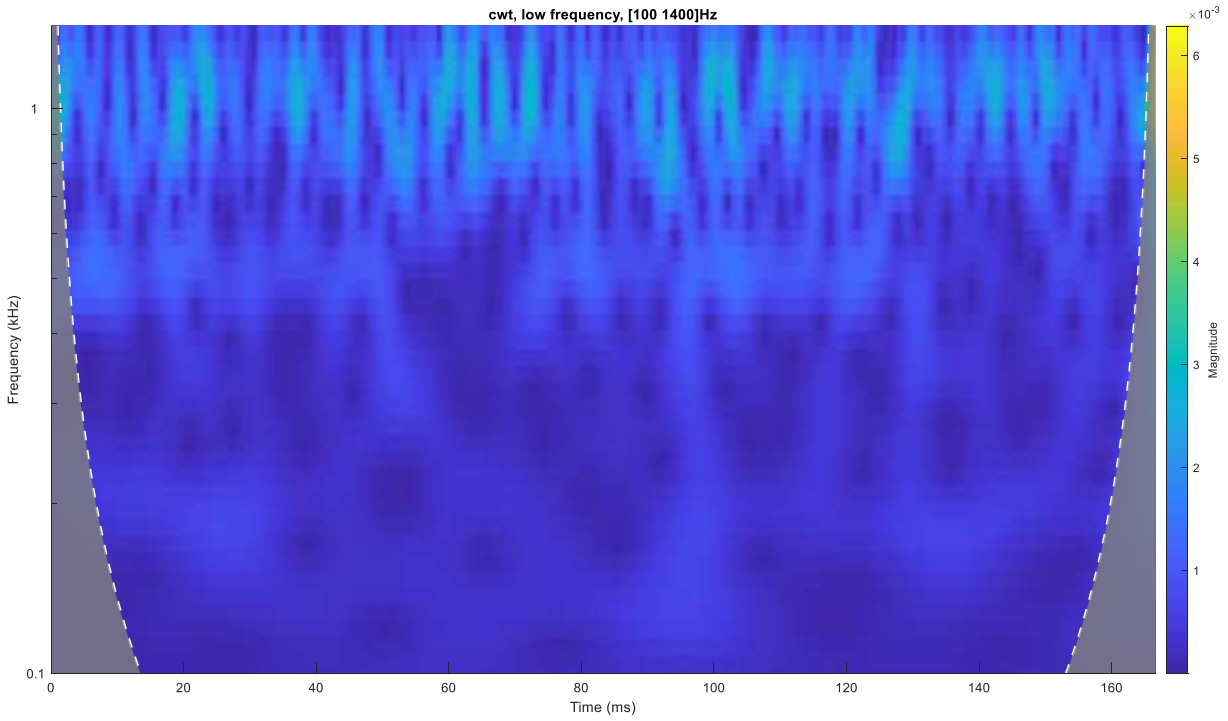

b) 100Hz-1400Hz band

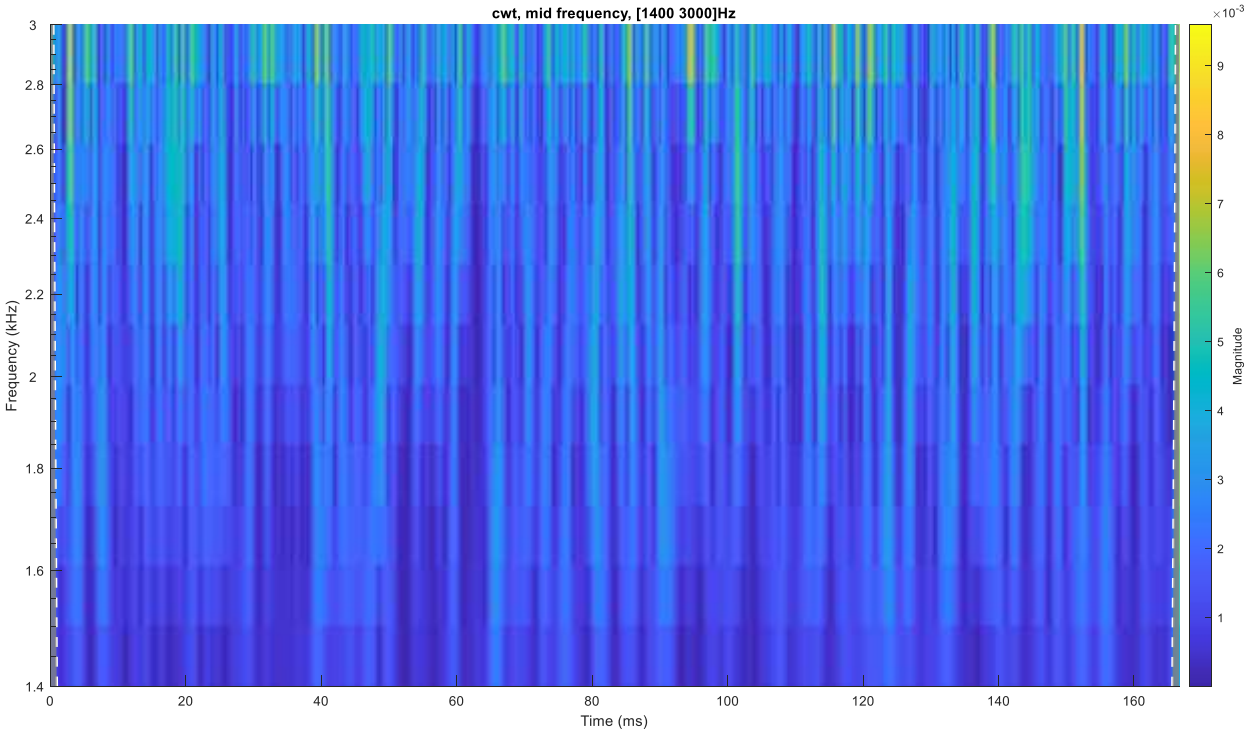

c) 1400Hz-3000Hz band

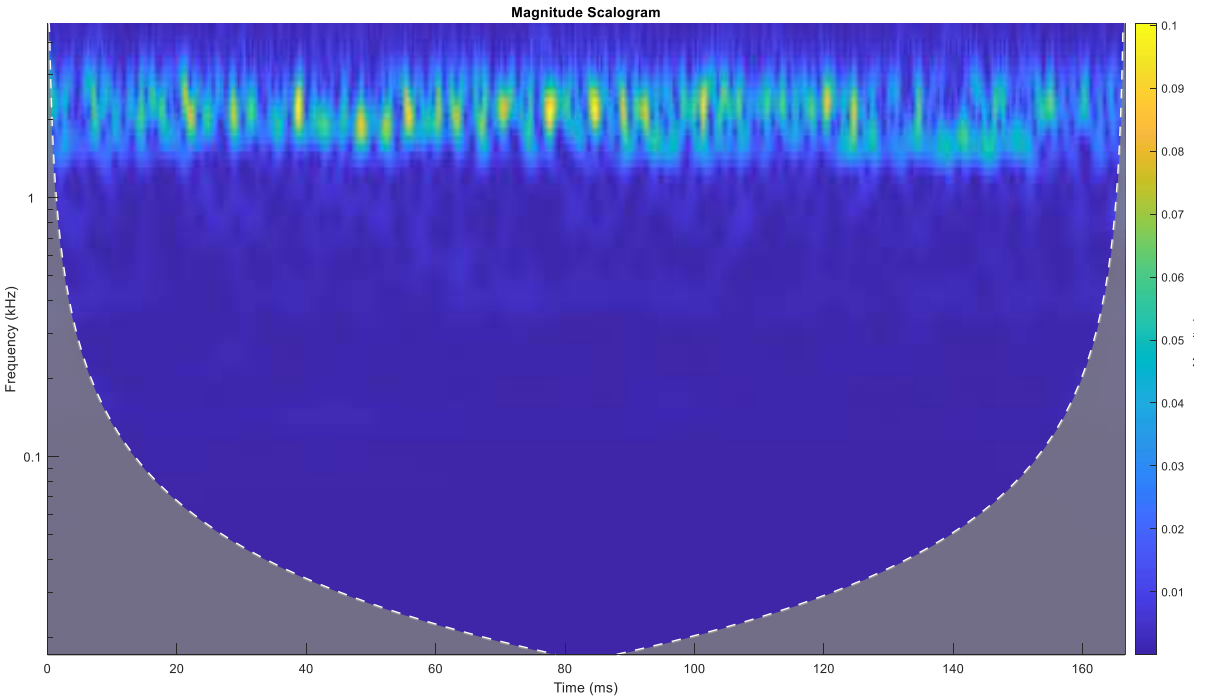

a) CWT of TSA pitted

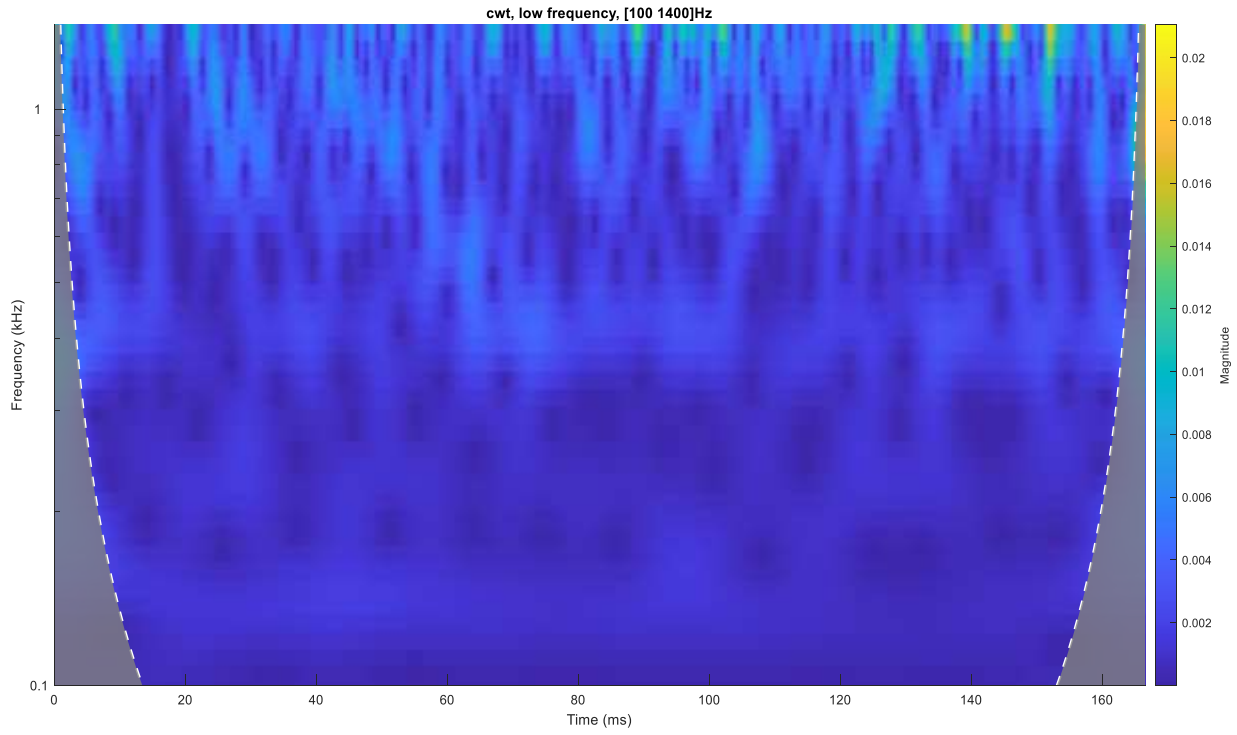

b) 100Hz-1400Hz band

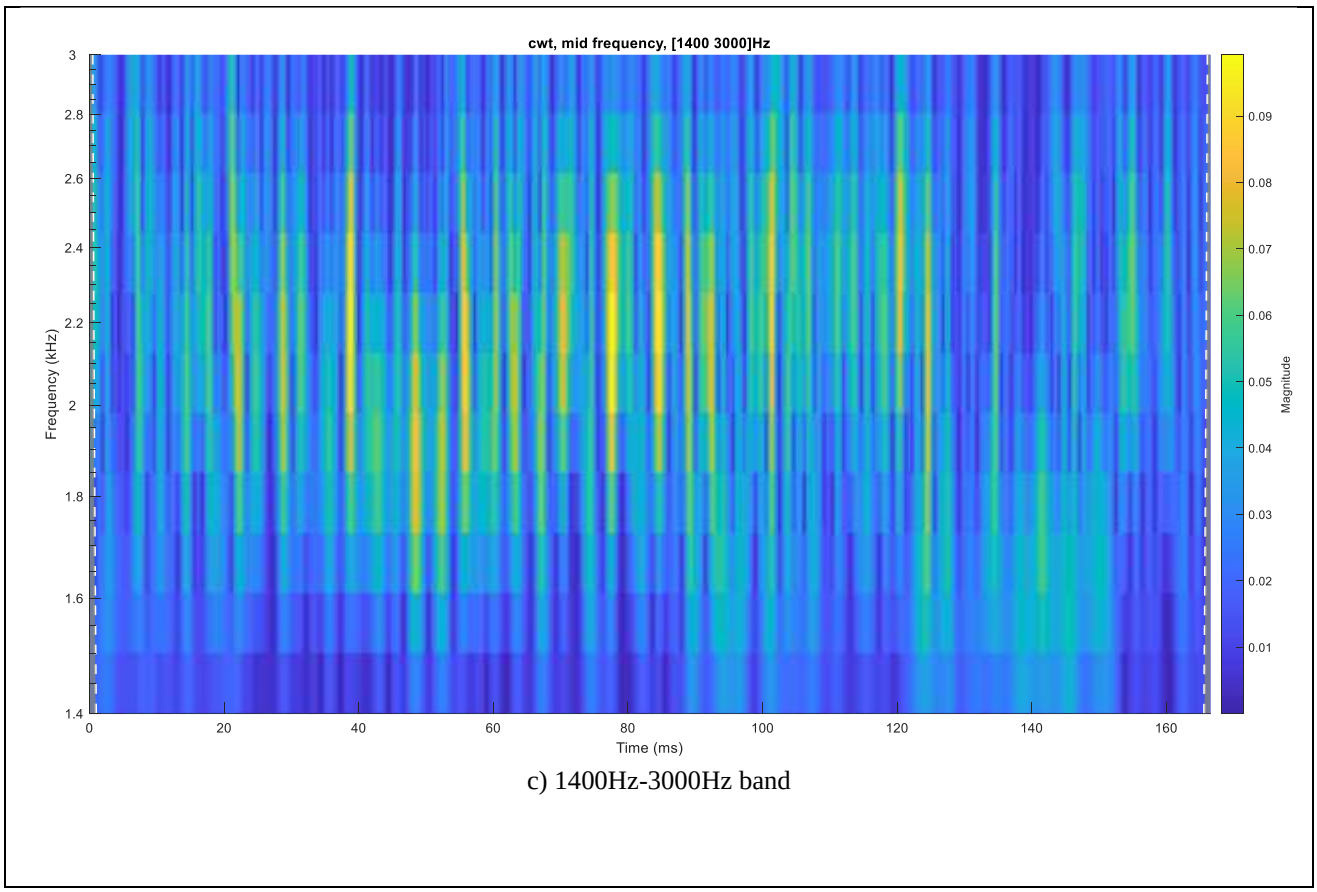

c) 1400Hz-3000Hz band

Fig. 22 Crack on tooth gearbox CWT of TSA acceleration

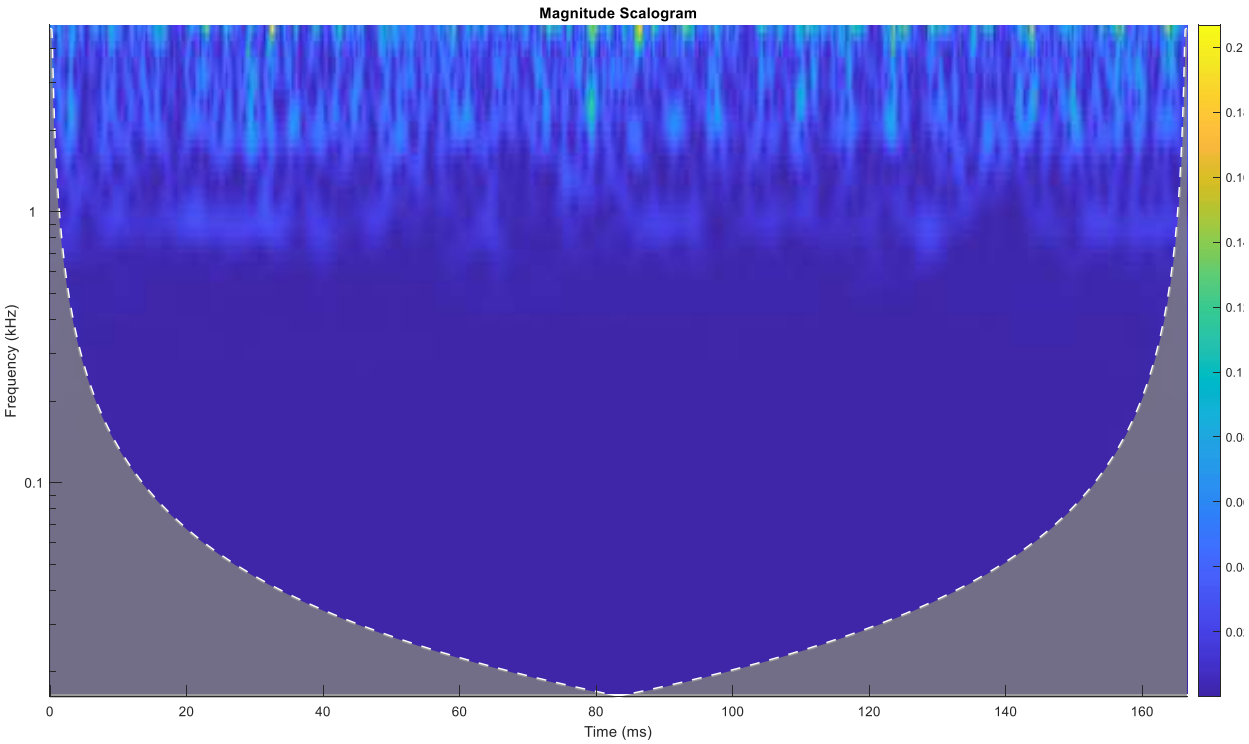

a) CWT of TSA crack on tooth

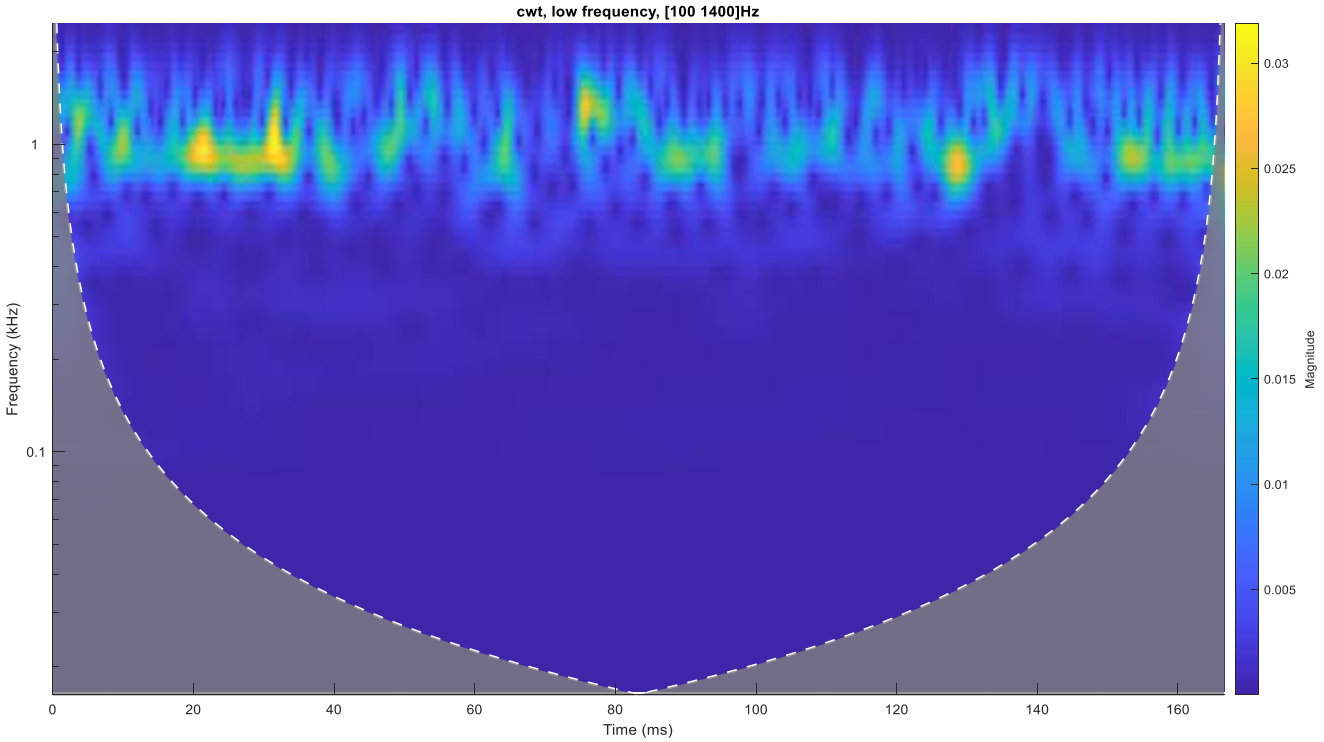

b) 100-1400 Hz band

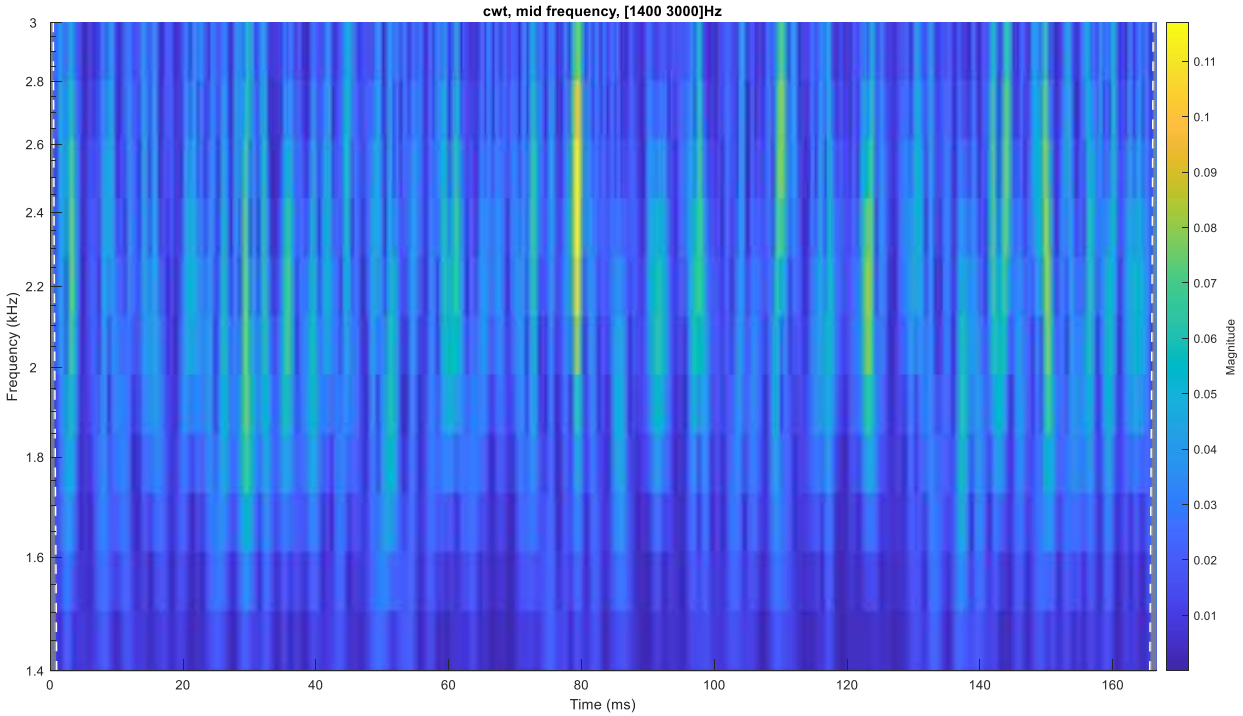

c) 1400-3000 Hz band

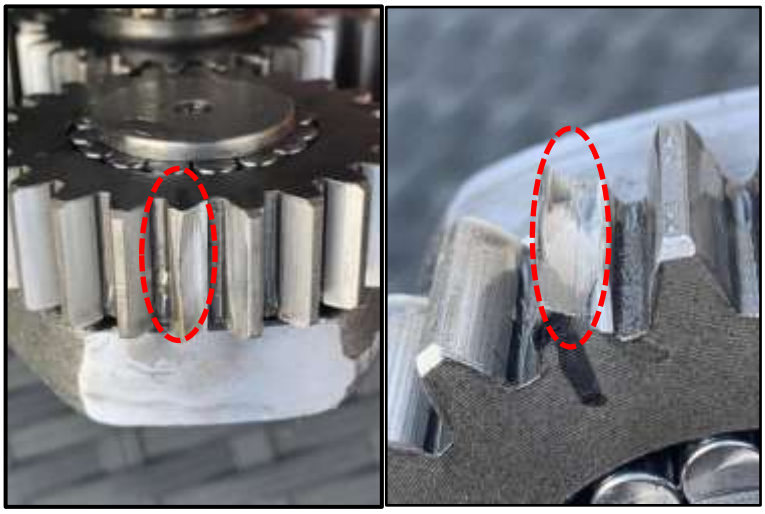

Fig 23 Crack on the planet tooth.

V. PROGNOSTICS

Failure prediction and severity of the gearbox are important safety factor in terms of reliability aspect. This section proposes a novel 6D model AR-K-Means algorithm for failure prediction that can detect the severity of fault or crack length on gears. K-means partitioning will cluster the information of data set and correlate the data based on center of gravity. This type of prognostics method can be used in many fields including machinery fault diagnostics to medical diagnostics. It is based on clustering the data into different subgroups and build a model for each subgroup to predict the probability of new coming data to belong to one of the clusters. The distribution of the system can then support prognostics by revealing the cause-and-effect relationship between the system and the wear level of components. Unlike supervised learning, clustering is considered an unsupervised learning method since we don't have the ground truth to compare the output of the clustering algorithm to the true labels to evaluate its performance.

The flow of algorithm is depicted in figure 24 for better understanding of the process. The method which is used in the fault prognosis part is based on k-means clustering method. Using this method, the given dataset is classified into k clusters based on the similarity among the data points. Algorithm can find the optimal number of clusters automatically as it is an unsupervised clustering method. However, in order to ease the fault prognosis task using the k-means, cluster numbers are chosen as $k = 4$, such that four severity levels can be identified, meaning low, medium, high and very high. Using the four levels, four clusters are obtained based on the given data. The input to the k-means model is a vector of features calculated at different severity level of tooth crack depth, starting from 0.2mm (low natural pitting in Fig.10) ranging to 4mm (crack in Fig.23). The feature vector includes NRMSE, SRA. SF and KV of the signals. Since the variables within a feature are of different magnitude order, the feature vector is normalized to the interval[0 1]. This results in better performance of the k-means model. The fault severity with respect to vibration collected over the different time period is illustrated in figure. 25 using spectral kurtosis. The spectral kurtosis (SK) is another statistical tool which can indicate the presence of series of transients and their locations in the frequency domain.After training the k-means model and forming the clusters, it is tested by assigning new dataset to check how it does the classification. For testing, a set of features associated with, low (0.2mm), medium (2.28mm) and very high (4mm) severity levels are given as inputs to the obtained k-means model. In order to understand, which cluster is related with which level of fault, a simple approach is to check the value of last column of the clusters. It is the AR norm and the higher the norm, the higher the severity level is. However, the fault prognosis algorithms is based on a feature vector and the fault severity is determined

using all of the components. Table 5, gives the centroids of the clusters. However, by checking the last column of the obtained clusters in table 6, it can be said that the cluster number 2, number 4, number 1, and number 3 corresponds to low, medium, high and very high severity levels, respectively. When the ID of the clusters assigned to the dataset (features) is checked, according to the table 5, the order of the cluster numbers, complies with the order of the dataset given to the k-means model. To clarify once more, the dataset is sorted based on increasing level of fault.

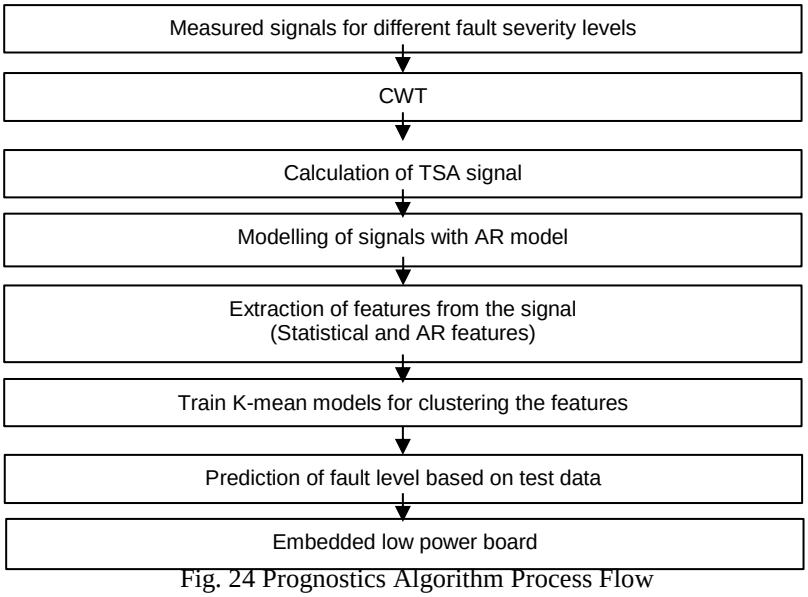

Fig. 24 Prognostics Algorithm Process Flow

Table 5. Clusters and their assignment

ID of the cluster Assigned	Cluster Centroids					
1	0.0952	0.3496	0.0343	0.5704	0.2900	0.8618
2	0.5788	0.9868	0.3622	0.0038	0.9796	0.1192
3	0.6805	0.0843	0.6034	0.9692	0.0600	0.9825
4	0.4017	0.7780	0.1715	0.1266	0.6939	0.5014

Table 6. Classification of clusters based on fault severity

Clusters assigned to test data	Test data					
4	0.3492	0.7113	0.1176	0.1782	0.6117	0.5764
1	0.2748	0.1957	0.2018	0.8314	0.1501	0.9833
3	0.9197	0.0199	0.8939	1.0000	0.0138	0.9427
3	0.9231	0.0191	0.8983	1.0000	0.0132	0.9419
3	0.9492	0.0125	0.9326	0.9995	0.0087	0.9352
3	0.9719	0.0069	0.9627	0.9985	0.0048	0.9290
3	0.9816	0.0045	0.9754	0.9980	0.0031	0.9264
3	0.9820	0.0044	0.9761	0.9980	0.0030	0.9263
3	0.9848	0.0037	0.9797	0.9978	0.0026	0.9255
3	0.9922	0.0019	0.9896	0.9974	0.0013	0.9235
3	1.0000	0	1.0000	0.9968	0	0.9213

In table 6, at the right column, each row shows the input feature vector and the left column the cluster to which it is assigned.

In the last part, a test dataset including medium, high and very high severity level is fed into the k-means model and the assigned clusters is checked. As it can be seen, according to the last column of table 6, the assigned clusters are true and this verifies the effectiveness of the k-means algorithms with the features extracted based on TSA signals. Although the developed algorithm for fault prognosis is based on experimental datasets, however, it can be effective when experimentally acquired data for different severity levels is available. In figure 25 (a-f), the trend of the extracted features with respect to fault severity level, i.e. crack depth is presented. Although all of the features do not have the same trend with respect to fault severity progress, however, a combination of the features gives better fault classification results. Further reduction of features can also be an alternative to reduce computational costs.

Fig. 25 Trends of features versus fault severity level

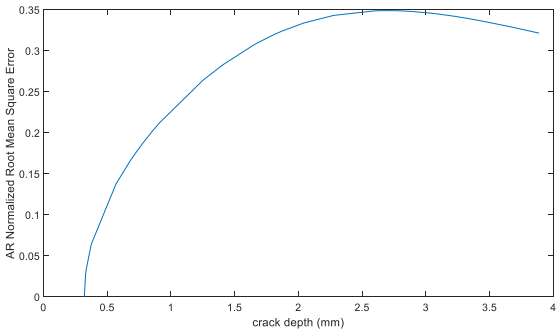

a- NRMSE

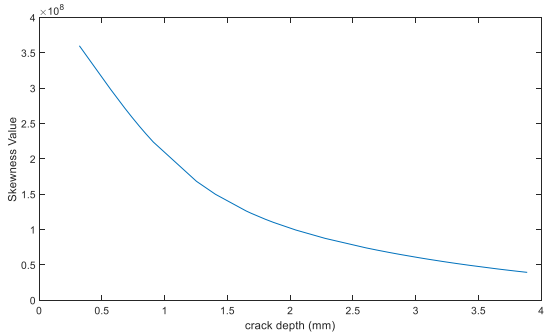

b- Skewness Values (SV)

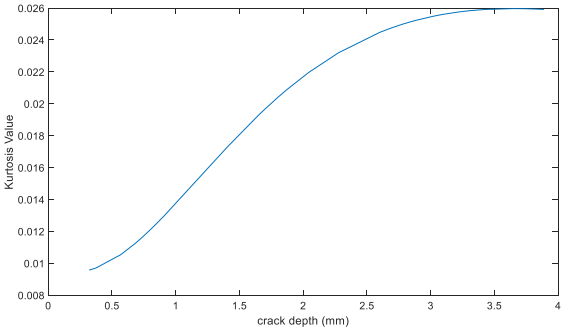

c-Kurtosis Value (KV)

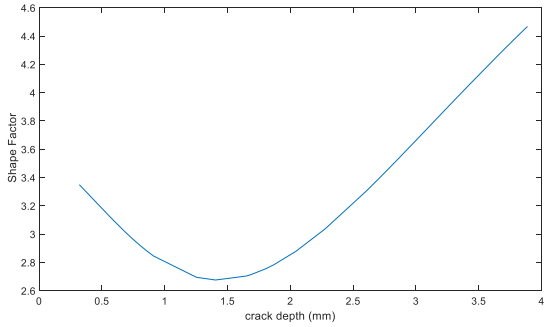

d- Shape Factor (SF)

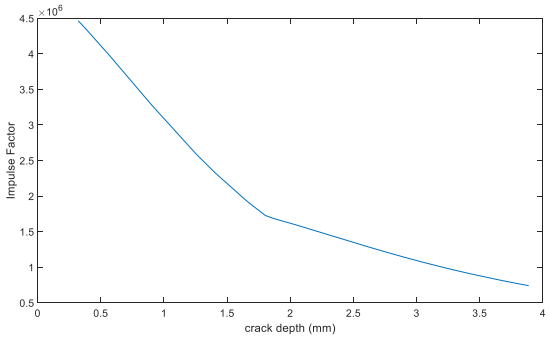

e-Impulse Factor (IF)

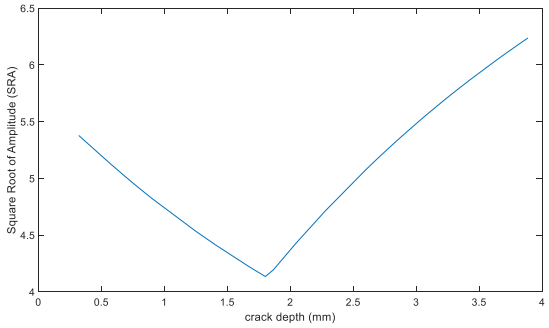

f- Square root of amplitude (SRA)

VI. DISCUSSION

This study has proposed a new milestone in planetary gearbox diagnostics using continuous wavelet transfer (CWT) for an effective FDD technique. CWT is efficient in treating transient events in the signal. The planetary gearbox's unique behavior is considerably challenging to study compared to other gearbox types. It possesses unique characteristic frequencies, making diagnostics even harder when there is a localized fault present in the system. All the analysis explained in the previous section shows interesting features of planetary gearbox characteristic frequencies, including mesh frequency and the frequency of gears and carrier and their sidebands (See Fig 17). The gear mesh frequency is clearly shown on the spectrum. Due to the ring gear error and carrier gear rotation effect, the modulation sidebands appear in the spectrum shown as a red dashed line (Fig.17). The planet's pass frequency causes asymmetric modulation sidebands around the gear mesh frequency and its harmonics. This effect is visible in the FFT spectrum (Fig 16, Fig 17). If there is a localized fault present in the planets, the defect will rotate with the speed of the carrier gear, and this rotational defect frequency can be named as f_d. The fault reveled itself by an increment in the amplitudes at the frequencies in an unhealthy gearbox ($f_m \; and \; f_m + nf_c \pm mf_p$) ($m = 1,2, \dots and \; n = 1,2, \dots$). Furthermore, the planet gear fault characteristics frequencies ($1f_p$ and $3f_p$) are prominent. All these observations accord the existence of a planet gear tooth fault.

The autoregressive model determined the NRMSE as an effective fault sensitive feature other than the statistical features SK, KV and SF of the signals. A change in the features indicates a change with respect to the healthy system, i.e. existence of a fault in the gearbox. The norm of the coefficients of the AR model of the signals showed itself as a reliable and effective feature in fault detection. The features are used as input to the K-means classifier, and the fault severity level is estimated effectively. According to this study, the faults in the planetary gearbox will produce impulses with respect to the planet-carrier cycle based on its fault type. For example, if a half tooth crack or root crack exists in the planets, it will produce eight impulses. And these impulses are due to the reduced mesh stiffness between the sun-planet and ring-planet mesh because of the crack.

In the same way, pitting causes impulses in the response. It has been found that the impulses produced by the pitted planet during the sun-planet mesh and ring-planet mesh are approximately spaced apart at equal distances. Whereas in the case of a tooth crack, the impulses produced by the planet-ring and planet-sun meshes are wide apart. The healthy gearbox impulses are feeble in the spectrum assuming that there is no faulty component in the spectrum. In contrast, the repetitive high impulses (See in Figure 21 c) are equispaced vertical lines corresponding to the planet carrier's rotating frequency (5.5 Hz). Finally, we took a close look at the lower impulses (See Figure 21 c) belonging to the planet gear's fault characteristics frequency (17 Hz). The crack on the planet tooth case CWT shows only high impulses at some periods which are wider apart, approximate to the planet's fault frequency $f_m \pm mf_p \pm nf_c$ (($m = 15 \; and \; n = 25$) (32 Hz , in Figure 22 c). This due to a crack on the tooth and a low contact ratio, as the teeth are not engaging properly. This indicates that there is a more prolonged effect on the system due to a distributed fault.

The proposed algorithm for fault classification and prognostics using the AR-K-means approach estimated the depth of crack and severity of the gearbox. This algorithm can reliably estimate the future condition of the gearbox by looking at all six-dimensional fault sensitive feature in case of pitting or crack present on the gear. When a new gearbox condition arises, the algorithm will automatically cluster the feature and indicate the fault level. If the fault level is above the safety threshold of the gearbox, replacement of the gear

component is essential. The final solution can be an embedded low power board that can sense vibrations continuously while the gearbox runs to reach a functional architecture.

VII. CONCLUSION

Planetary gearbox condition monitoring is essential due to its criticality in wind turbines, helicopters and automotive transmission systems. Hence, its reliability, maintainability and availability are significant. In addition, predictive maintenance is essential to avoid downtime in critical mechanical systems.

The failure of planet gears and bearings have been much reported over time. Due to the failure of planet gears in the gearbox, the planets were for this study. This research proposed a fault detection and diagnostics tool for a planetary gearbox in different fault conditions using continuous wavelet transform and AR modelling. The vibration signals have been captured from a single-stage spur planetary gearbox test rig in different fault conditions and analysed using AR modelling, FFT and envelop analysis. The fault is confirmed in the presence of the fault frequencies, high harmonics at multiples of gear mesh frequencies and high KV and NRMSE values. To ensure the fault type and the affected component, the continuous wavelet transform scalogram has been used by analysing the fault frequency impulses with respect to time. Both the localised and distributed fault impulses have been identified using the CWT scalogram. This illustrates the effectiveness of the CWT- AR diagnosis method for the diagnosis and extraction of fault features of non-stationary planetary gearbox signals. The fault classification and prognostics of the gearbox using the AR-K-means approach are developed for estimating the fault severity and future state of the gearbox. In addition, the AR-K-means hybrid methodology for the planetary gearbox is devised to forecast the increase in the level of crack length on planet gear in the planetary gearbox.

Although the CWT, AR and K-means methods have been vastly used in the literature, the way that especially CWT is used in this work is different. Based on the fault feature appearance in the CWT in the fault detection step, the signals are reconstructed to include only certain frequency bands that carry valuable information about the fault rather than taking the signal in its raw form. Furthermore, the AR approach models the signal and finds the partial dynamics of the gearbox embedded in the response, which makes it sensitive to a change in the system due to a fault. Therefore, it adds to the efficacy of the fault diagnosis algorithm. The experimental study results indicate that this prognostics approach has high accuracy in predicting future fatigue crack on planet gear.

REFERENCES

[1] Hong, L., Qu, Y., Tan, Y., Liu, M. and Zhou, Z. Vibration Based Diagnosis for Planetary Gearboxes Using an Analytical Model. Shock and Vibration. 2016: 1-11.

[2] Berlato, F., D'Elia, G., Battarra, M. and Dalpiaz, G. Condition monitoring indicators for pitting detection in planetary gear units. Diagnostyka. 2020; 21(1): 3-10.

[3] Zhou, G., Zuo, C., Wang J. and Liu S. Gearbox Fault Diagnosis Based on Wavelet-AR Model. 2007 International Conference on Machine Learning and Cybernetics; 19-22 August 2007, Hong Kong; 2007: 1061-1065.

[4] Wang, D., Tsui, K. and Miao, Q. Prognostics and Health Management: A Review of Vibration Based Bearing and Gear Health Indicators. IEEE Access. 2018; 6: 665-676.

[5] Miao, Q. and Zhou, Q. Planetary Gearbox Vibration Signal Characteristics Analysis and Fault Diagnosis. Shock and Vibration. 2015: 1-8.

[6] Li, Z., Yan, X., Yuan, C., Peng, Z. and Li, L. Virtual prototype and experimental research on gear multi-fault diagnosis using wavelet-autoregressive model and principal component analysis method. Mechanical Systems and Signal Processing. 2011; 25(7): 2589-2607.

[7] Assaad, B., Eltabach, M. and Antoni, J. Vibration based condition monitoring of a multistage epicyclic gearbox in lifting cranes. Mechanical Systems and Signal Processing. 2014; 42(1-2): 351-367.

[8] Al-Badour, F., Sunar, M. and Cheded, L. Vibration analysis of rotating machinery using time–frequency analysis and wavelet techniques. Mechanical Systems and Signal Processing. 2011; 25(6): 2083-2101.

[9] Vernekar, K., Kumar, H. and Gangadharan, K. Gear Fault Detection Using Vibration Analysis and Continuous Wavelet Transform. Procedia Materials Science. 2014; 5: 1846-1852.

[10] Wu, J. and Chen, J. Continuous wavelet transform technique for fault signal diagnosis of internal combustion engines. NDT & E International. 2006; 39(4): 304-311.

[11] Tse, P., Yang, W. and Tam, H. Machine fault diagnosis through an effective exact wavelet analysis. Journal of Sound and Vibration. 2004; 277(4-5):1005-1024.

[12] Saravanan, N. and Ramachandran, K. Incipient gear box fault diagnosis using discrete wavelet transform (DWT) for feature extraction and classification using artificial neural network (ANN). Expert Systems with Applications. 2010; 37(6): 4168-4181.

[13] Wang, X. and Makis, V. Autoregressive model-based gear shaft fault diagnosis using the Kolmogorov–Smirnov test. Journal of Sound and Vibration. 2009; 327(3-5): 413-423.

[14] Baillie, D. and Mathew, J. A comparison of autoregressive modeling techniques for fault diagnosis of rolling element bearings. Mechanical Systems and Signal Processing. 2996; 10(1): 1-17.

[15] Wang, W. and Wong, A. Autoregressive Model-Based Gear Fault Diagnosis. Journal of Vibration and Acoustics. 2002; 124(2): 172-179.

[16] Rafiee, J., Rafiee, M. and Tse, P. Application of mother wavelet functions for automatic gear and bearing fault diagnosis. Expert Systems with Applications. 2010; 37(6): 4568-4579.

[17] Samanta, B. Gear fault detection using artificial neural networks and support vector machines with genetic algorithms. Mechanical Systems and Signal Processing. 2004; 18(3): 625-644.

[18] Rafiee, J. and Tse, P. Use of autocorrelation of wavelet coefficients for fault diagnosis. Mechanical Systems and Signal Processing. 2009; 23(5): 1554-1572.

[19] Sun, Q. and Tang, Y. Singularity analysis using continuous wavelet transform for bearing fault diagnosis. Mechanical Systems and Signal Processing. 2002; 16(6): 1025-1041.

[20] Bendjama, H., Bouhouche, S. and Boucherit, M. Application of Wavelet Transform for Fault Diagnosis in Rotating Machinery. International Journal of Machine Learning and Computing. 2012: 82-87.

[21] Barbieri, N., de Sant'Anna Vitor Barbieri, G., Martins, B., de Sant'Anna Vitor Barbieri, L. and de Lima, K. Analysis of automotive gearbox faults using vibration signal. Mechanical Systems and Signal Processing. 2019; 129: 148-163.

[22] Dalpiaz, G., Rivola, A. and Rubini, R. Effectiveness and sensitivity of vibration processing techniques for local fault detection in gears. Mechanical Systems and Signal Processing. 2000; 14(3): 387-412.

[23] Wang, W., Ismail, F. and Farid Golnaraghi, M. Assessment of gear damage monitoring techniques using vibration measurements. Mechanical Systems and Signal Processing. 2001; 15(5): 905-922.

[24] Al-Bugharbee, H. and Trendafilova, I. Autoregressive modelling for rolling element bearing fault diagnosis. Journal of Physics: Conference Series. 2015; 628: 012088.

[25] Ayaz, E. Autoregressive modeling approach of vibration data for bearing fault diagnosis in electric motors. Journal of Vibroengineering. 2014; 16(5): 2130-2138.

[26] Nikhar, N., Patankar, S. and Kulkarni, J. Gear tooth fault detection by autoregressive modelling. Fourth International Conference on Computing, Communications and Networking Technologies (ICCCNT); July 4-6 2013, Tiruchengode, Tamil Nadu, India; 2013.

[27] Zheng, H., Li, Z. and Chen, X. Gear fault diagnosis based on continuous wavelet transform. Mechanical Systems and Signal Processing. 2002; 16(2-3): 447-457.

[28] Chang, S., Bin Yu and Vetterli, M. Adaptive wavelet thresholding for image denoising and compression. IEEE Transactions on Image Processing. 2000; 9(9): 1532-1546.

[29] Rioul, O. and Duhamel, P. Fast algorithms for discrete and continuous wavelet transforms. IEEE Transactions on Information Theory. 1992; 38(2): 569-586.

[30] Jafarizadeh, M., Hassannejad, R., Ettefagh, M. and Chitsaz, S. Asynchronous input gear damage diagnosis using time averaging and wavelet filtering. Mechanical Systems and Signal Processing. 2008; 22(1): 172-201.

[31] Merry, R. J. E. Wavelet theory and applications: a literature study. DCT rapporten: Technische Universiteit Eindhoven. 2005; 2005.053.

[32] Kay, S. Modern Spectral Estimation. Englewood Cliffs, N.J: Prentice Hall; 1988: 106-120.

[33] Miao, Q. and Zhou, Q.Planetary Gearbox Vibration Signal Characteristics Analysis and Fault Diagnosis. Shock and Vibration. 2015: 1-8.

[34] Feng, Z., Zhang, D. and Zuo, M. Planetary Gearbox Fault diagnosis via Joint Amplitude and Frequency Demodulation Analysis Based on Variational Mode Decomposition. Applied Sciences. 2017; 7(8): 775.

[35] Pattabiraman, T.R., Srinivasen, K. and Malarmohan, K. Assessment of sideband energy ratio technique in detection of wind turbine gear defects. Case Studies in Mechanical Systems and Signal Processing. 2015; 2: 1-11.

[36] Zhang, M., Wang, K., Wei, D. and Zuo, M. Amplitudes of characteristic frequencies for fault diagnosis of planetary gearbox. Journal of Sound and Vibration. 2018; 432: 119-132.

[37] Hong, L. and Dhupia, J. Vibration Signal Modulation of Equally Spaced Planetary Gear-set with Gear Tooth Faults. Proceedings of the 8th International Conference on Structural Dynamics. 2011: 2156-2162.

[38] Li, Y., Ding, K., He, G. and Yang, X. Vibration modulation sidebands mechanisms of equally-spaced planetary gear train with a floating sun gear. Mechanical Systems and Signal Processing. 2019; 129: 70-90.

[39] Elasha, F., Greaves, M. and Mba, D. Planetary bearing defect detection in a commercial helicopter main gearbox with vibration and acoustic emission. Structural Health Monitoring. 2018; 17(5): 1192-1212.

[40] Antoni, J. and Randall, R. Unsupervised noise cancellation for vibration signals: part I—evaluation of adaptive algorithms. Mechanical Systems and Signal Processing. 2004; 18(1): 89-101.

[41] Huff, E. and Tumer, I. Using triaxial accelerometer data for vibration monitoring of helicopter gearboxes. Journal of Vibration and Acoustics. 2003; 128(4): 120–128.

[42] Sawalhi, N. Vibration Sideband Modulations and Harmonics Separation of a Planetary Helicopter Gearbox with Two Different Configurations. Advances in Acoustics and Vibration. 2016: 1–9.

[43] Zhang, H., Qi, C., Fan, J., Dai, S. and You, B. Vibration Characteristics Analysis of Planetary Gears with a Multi-Clearance Coupling in Space Mechanism. Energies. 2018; 11(10): 2687.

[44] Zhou, J., Sun, W. and Cao, L. Vibration and noise characteristics of a gear reducer under different operation conditions. Journal of Low Frequency Noise, Vibration and Active Control. 2018; 38(2): 574–591.

[45] Guo, Y., Zhao, L., Wu, X. and Na, J. Vibration separation technique based localized tooth fault detection of planetary gear sets: A tutorial. Mechanical Systems and Signal Processing. 2019; 129: 130–147.

[46] Yang, Q., Liu, C., Zhang, D. and Wu, D. (2012). A New Ensemble Fault Diagnosis Method Based on K-means Algorithm. International Journal of Intelligent Engineering and Systems, 5(2), pp.9–16.

[47] Amruthnath, N. and Gupta, T. (2019). Fault Diagnosis Using Clustering. What Statistical Test to use for Hypothesis Testing? Machine Learning and Applications: An International Journal, 6(1), pp.17–33.

[48] Elattar, H.M., Elminir, H.K. and Riad, A.M. (2016). Prognostics: a literature review. Complex & Intelligent Systems, 2(2), pp.125–154.

[49] Teng, W., Zhang, X., Liu, Y., Kusiak, A. and Ma, Z. (2016). Prognosis of the Remaining Useful Life of Bearings in a Wind Turbine Gearbox. Energies, 10(1), p.32.

[50] Elasha, F., Mba, D., Togneri, M., Masters, I. and Teixeira, J.A. (2017). A hybrid prognostic methodology for tidal turbine gearboxes. Renewable Energy, 114, pp.1051–1061.

[51] Yu, Jing & Makis, Viliam. (2011). Wavelet analysis with time-synchronous averaging of planetary gearbox vibration data for fault detection and diagnostics. 10.1109/CSAE.2011.5953252.

[52] Guo, J., Shi, Z., Li, H., Zhen, D., Gu, F., & Ball, A. D. (2018). Early Fault Diagnosis for Planetary Gearbox Based Wavelet Packet Energy and Modulation Signal Bispectrum Analysis. Sensors (Basel, Switzerland), 18(9), 2908. https://doi.org/10.3390/s18092908